FLAT RING EMITTER ELECTRON GUNS

A STUDY OF FLAT RING EMITTER ELECTRON GUNS

by

Stanley B. Harvey, B. Eng.

PART B: MCMASTER (OFF CAMPUS) PROJECT*

A Report Submitted to the School of Graduate Studies
in Partial Fulfilment of the Requirements
for the Degree
Master of Engineering

Department of Engineering Physics
McMaster University
Hamilton, Ontario, Canada

September, 1976

* One of the two Project Reports: The other part is designated PART A: ON CAMPUS PROJECT

MASTER OF ENGINEERING (1976) MCMASTER UNIVERSITY

Engineering Physics Hamilton, Ontario

TITLE: A STUDY OF FLAT RING EMITTER ELECTRON GUNS

AUTHOR: STANLEY BROOKS HARVEY, B.Eng. (McMaster University)

SUPERVISOR: Dr. R.M. Hutcheon (Chalk River Nuclear Laboratories, Atomic Energy of Canada Limited)

NUMBER OF PAGES: ii, 50.

ABSTRACT

The design and performance of a flat emitting ring on-axis electron gun suitable for use in a small reflected beam accelerator was investigated. The design constraints include a low emittance (approximately 5π cm mrad), and a small beam size with a focus approximately 13 cm from the emitting surface.

A suitable geometry was determined theoretically and was tested with a dispenser cathode. A beam with a focus at 12.7 $\pm$ 1 cm and an emittance of approximately 7π cm mrad was obtained. However, the dispenser cathode response time to heater current changes is too large for the required gun current control.

Experiments were done to study the mechanical and thermal properties of flat emitting foil rings, since a directly heated foil has a fast response time. Two foils were tested: 1.27×10^{-3} cm thick tungsten and 4.57×10^{-4} cm thick tantalum. The present simple design requires impractically thin foils ($\leq$ 0.25 microns thick) to reach emission temperatures at feasible heater currents.

ACKNOWLEDGEMENTS

The author wishes to express his appreciation to Dr. R.M. Hutcheon for his patient guidance and constant support of this study. The National Research Council of Canada post-graduate scholarship which helped to fund this work is gratefully acknowledged.

TABLE OF CONTENTS

Table of Contents: Cont'd

1. INTRODUCTION

1.1 The Medical Accelerator

There is an increasing demand for compact variable energy electron accelerators for use in both photon and electron mode cancer treatment. Such an accelerator must be economical and at the same time conform to the stringent standards and specifications of hospitals. The electron current and energy must be constant for each treatment over periods of up to five minutes and must be variable between treatments. To obtain the necessary photon dose rates of 30 to 300 Rads per minute at a metre requires electron beams of up to 400 mA.

The electron accelerator being developed by Chalk River Nuclear Laboratories basically consists of an electron gun, a linear accelerating coupled rf cavity structure, an electron beam reflecting magnet and a bremsstrahlung target system with deflection magnet. The reflecting magnet allows the beam to be reinjected and accelerated again by the rf cavities thus minimizing the overall unit length and reducing rf power requirements. The electron output energy is variable between 5 and 25 MeV by changing the reinjection phase.

The accelerator is approximately 1.6 m long and the beam drift tubes are of 1 cm inside diameter. Electrons which are lost by striking the walls are a waste of rf power and produce unwanted radiation both of which increase the cost of a medical unit. Thus the optimization of the electron gun design is very important.

An on-axis cathode configuration was chosen to avoid the increased complexity of off-axis injection. After making the second pass through the rf cavities, the beam must exit from the system through a central hole in the gun. Thus a hollow cathode, annular gun is required. Although the technology of electron beam production from planar or spherical sources is well documented(1-4), the perturbations of the electric field caused by a hole in the emitting surface have not been studied in the past.

The annular guns designed to date have used a bifilar thoriated tungsten filament wound in a ring as the emitting surface. The curvature of the electric field around the emitting wires tends to give the electrons an unwanted velocity component perpendicular to the gun axis. In this configuration it is difficult to make the emittance acceptably small. Better beam optics should be achieved by using a flat ring emitter from which the electrons would leave normal to the surface with only small edge perturbations. This paper is the result of a study of flat ring emitters conducted at the Chalk River Nuclear Laboratories of Atomic Energy of Canada Limited.

1.2 Choice of Emitters

A wide variety of electron emitters is available but only a few are suitable for this present application. The materials must be compatible with use in vacuum and have low outgassing rates at the high operating temperatures. Filaments must have good mechanical rigidity since the accelerator package is to be rotated through 360°. Emitters must be able to operate for 10,000 hours in pressures up to 1×10^{-4} P. Commercial availability of the emitting material is also desirable. The following sections summarize the advantages and shortcomings of some of the more common types of thermionic emitters.

1.2.1 Pure Metals

All clean metals will emit electrons if heated to a sufficient temperature. To be of value, however, the metal must produce the required emission without evaporating too rapidly. Jenkins[5] states that a vapour pressure of 10^{-5} P is generally considered acceptable which restricts the useful metals to tungsten, tantalum and rhenium. The pure metals can function under poor vacuum conditions because of their high operating temperature but for the same reason their power dissipation is large. The emission current density of tungsten at 1700°C is only 0.3 mA/cm^2 [6].

1.2.2 Oxide Coating

The oxide coated cathodes are composed of barium oxide, strontium oxide or both deposited on a nickel base. Buttons of oxide may also be used and heated indirectly. Emission densities of 0.5 A/cm^2 are possible at the relatively low temperatures in the range 725 - 825°C. Overheating the cathode will severely reduce its life and oxidizing gas partial pressures must be lower than 10^{-5} P to avoid poisoning. The basic coatings are particularly susceptible to damage by positive ion bombardment and arcing so many modifications exist to make the oxide cathodes more suitable for specific high power applications. A disadvantage of oxide cathode is the low emission efficiency (mA/watt) for a given current density.

1.2.3 Metals with an Electropositive Monolayer

A surface monolayer of an electropositive element increases electron emission by reducing the work function of the metal substrate on which it is deposited. Although tantalum and rehnium substrates can be used, the most common is tungsten because it is both strong and inexpensive.

The monolayer is generally very stable yet there must be some reservoir to replace surface atoms which are evaporated or sputtered away. This is usually accomplished by incorporating the monolayer material as an impurity in the substrate and allowing it to diffuse to the surface slowly. The most common monolayers are thorium and barium.

Thoriated Tungsten

Tungsten wire with approximately 1% thorium oxide added has proven to be a suitable emitter in gun tests conducted to date. As the emitter is directly heated, the relative emission efficiency is good. Ayer[7] points out that by "carburizing" the filament (i.e. forming a layer of tungsten carbide on the surface) a further 60-70% power reduction is realized which lowers the cost of the pulse transformer.

Carburization has other advantages including reduced susceptability to deactivation by positive ion bombardment and a thorium evaporation rate of one-sixth that of the pure metal[8]. Life times are commonly over 20,000 hours[7] and may extend to 50,000 hours[8]. The carburizing is accomplished by heating the filament in a hydrogen-hydrocarbon atmosphere for a time dependent on the amount of carburization desired.

The filaments require an initial activating heat cycle after which operating temperatures are between 1500 and 1700°C for 500 to 2000 mA/cm^2. Emission densities of up to 10 A/cm^2 are possible.

The carburized filaments can operate at 1700°C in pressures of 10^{-3} P. Poisoning causes depletion of the carbide but recovery is possible providing that some carbide remains[9].

1.2.4 Dispenser Cathode

The thin emitting film of a dispenser cathode is maintained by the evolution of barium through a porous tungsten reservoir. The tungsten is impregnated with various ratios of BaO, CaO and Al_2O_3. Unlike the monolayer in the case of thoriated tungsten, the dispenser cathode is covered with a thin barium surface layer randomly dotted with thicker patches of barium[10]. This surface is produced by a carefully controlled heat treatment procedure.

The dispenser cathodes are characteristically high current density emitters with several amps per square centimeter being typical. There are several basic types[5, 8,12,13], varying in method fabrication, relative proportions of impregnant constituents, current density, operating temperature, life expentancy and susceptability to poisoning. All dispenser cathodes suffer from poisoning by oxygen at partial pressures in excess of 10^{-5} P[8]. The operating temperature range is 900°C to 1100°C. Emission density must be traded off against lifetime but for the currents required in this application, the lifetime is expected to be much longer than the design value of 10,000 hours.

1.2.5 Other Thermionic Emitters

There are many other electron sources which have been used for various applications. Some are listed in Table 1 but all were deemed unsuitable for the application under consideration.

It was decided that thoriated tungsten was the best emitter choice for this particular application. However, since the only major problem with the dispenser cathode was the requirement of a lower than presently attainable pressure within the accelerator, and because improved handling techniques may improve this, a study of dispenser type devices was considered to be warranted.

TABLE 1

OTHER EMITTERS

Emitter	Major Disadvantage
Caesim on tungsten(5,13,14)	- not vacuum compatible
Lanthanum hexaboride(15,16,17)	- technical problems associated with fabrication
Barium zirconate(18)	- requires electric discharge to achieve high density
Thoria coated iridium wire(19)	- still under development

2. ELECTRON GUN OPTICS

2.1 Constraints

For reasons of economy, both the electron gun and the magnetron (which supplies the S band rf power) are powered by the same modulator and pulse transformer. Thus the gun high voltage pulse is 42 kV for 4 μsec duration as determined by the magnetron operating characteristics.

Figure 1 shows the gun, focus coil and the first two rf cells of the accelerator. Beam dynamics calculations[20] have shown that the electrons must be focused at the entrance to cell #2 to achieve maximum transmission. Thus the electron guns were designed to have a focus approximately 13 cm from the anode nose by selecting suitable anode and wehnelt shapes and sizes, and focus coil strengths.

An estimate of the required beam emittance can be obtained from consideration of the electron trajectories through the accelerator in a 42 keV frame of reference (Figure 2), i.e. in the injection frame. It is assumed that emittance is conserved in this frame which is essentially a rest frame. The path lengths shown are for a beam of 12.5 MeV at the reflecting magnet and 5 MeV at the target. The two high energy focus coils shown in this unfolded accelerator view are really the same coil as seen twice by the beam.

Calculations[20] show that a 300 mA beam injected into the accelerator with a diameter of 9.2 mm, a maximum convergence angle of 2.4 degrees, and an emittance envelope of π 5cm mrad (2.8 mm deg.) can be completely transmitted through both passes. Space charge and defocusing effects of the rf cells were considered in the calculation. The emittance is fundamentally determined by the electron trajectories between the cathode and anode.

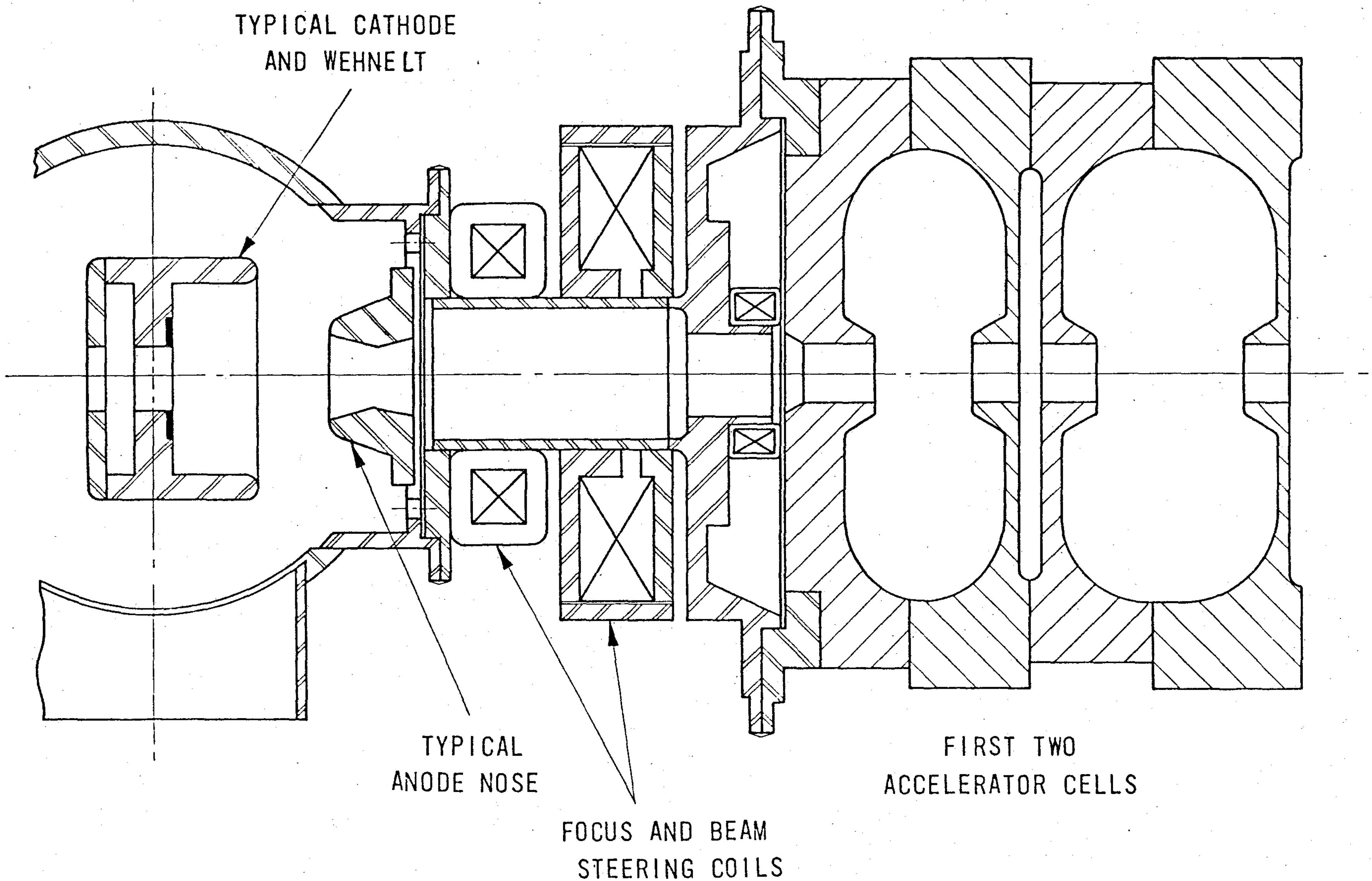

Fig. 1: Cross-sectional view of accelerator injection end showing electron gun, focus coil and first two rf cells.

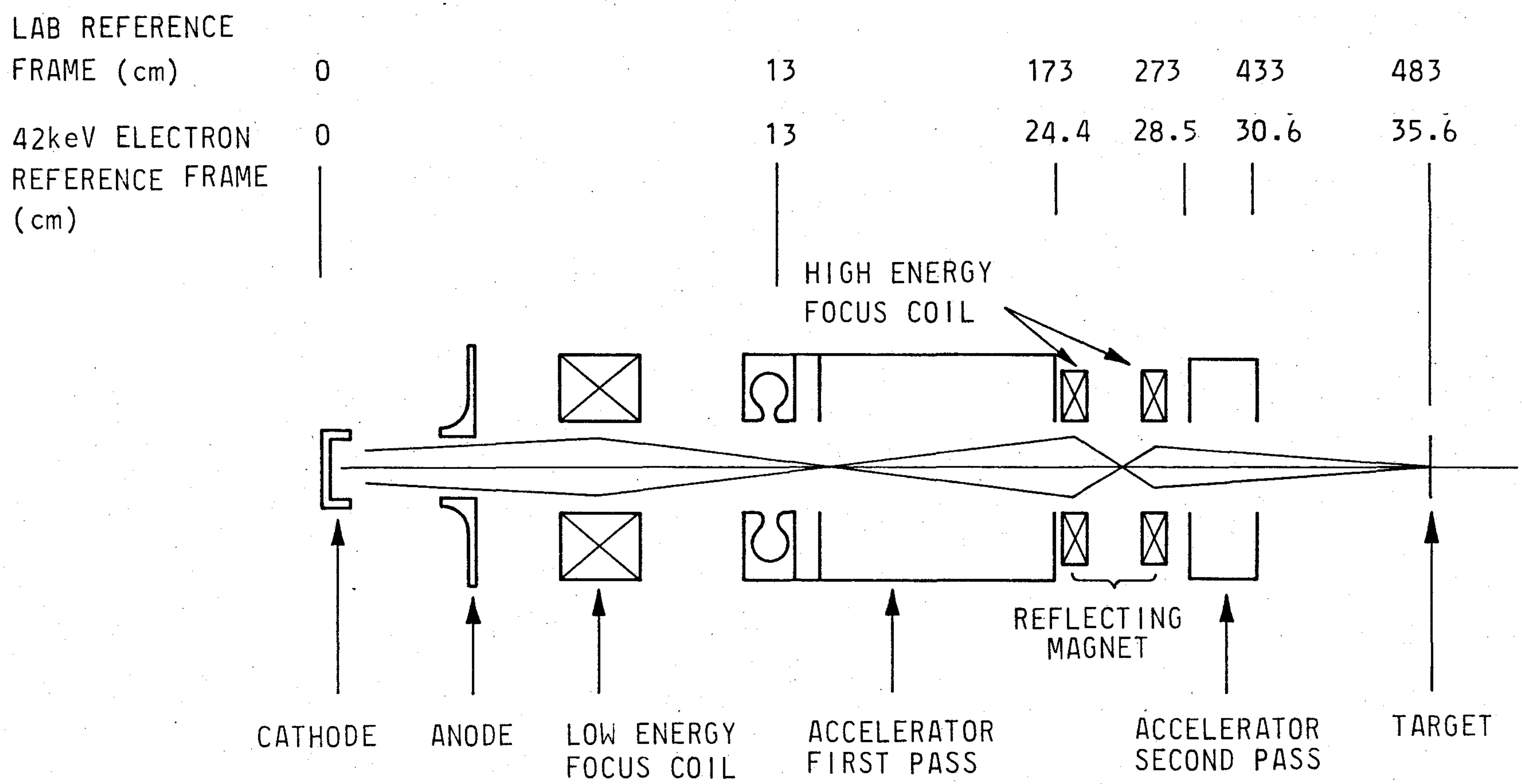

Fig. 2. Schematic representation of the accelerator system in laboratory frame and in a reference frame where the electron has an energy of 42 keV. The proposed optics are represented by the trajectories shown.

2.2 Trajectories

The SLAC[21] computer code was used to determine equipotential lines and electron trajectories between given shapes of cathode and anode. Wehnelt length, emitter geometry, anode-cathode separation, and anode nose length and diameter can be modified to determine the effect on beam diameter. Figures 3 and 4 are computer plots of a configuration similar to that used in these gun tests. Equipotential lines and selected trajectories are shown. The latter are to be compared with Figure 5 which is for the same geometry but using a bifilar filament instead of the planar source. The advantages of the ring emitter are apparent.

It is desirable to have a nearly parallel beam entering the focus coil, which is located approximately 7 cm from the emitting surface. The trajectories of Figure 3 achieve this condition and thus reduce the focus coil power dissipation and optical aberations.

Increasing the wehnelt cylinder length (dimension A in Figure 6) increases the curvature of the equipotentials and causes the beam to be more convergent, although a large wehnelt change is required for any noticeable beam compression. As the anode to cathode spacing (dimension B in Figure 6) becomes smaller, the equipotential lines are bent more and the beam converges less rapidly. The anode hole behaves like a diverging lense with a focal length given by Pierce[3] as

$$f = \frac{-4V}{V'}$$

for V = anode voltage

V' = gradient on upstream side of anode.

An estimate from Figure 4 gives a voltage gradient of 55 kV/cm. With V = 42 kV, f = -3 cm.

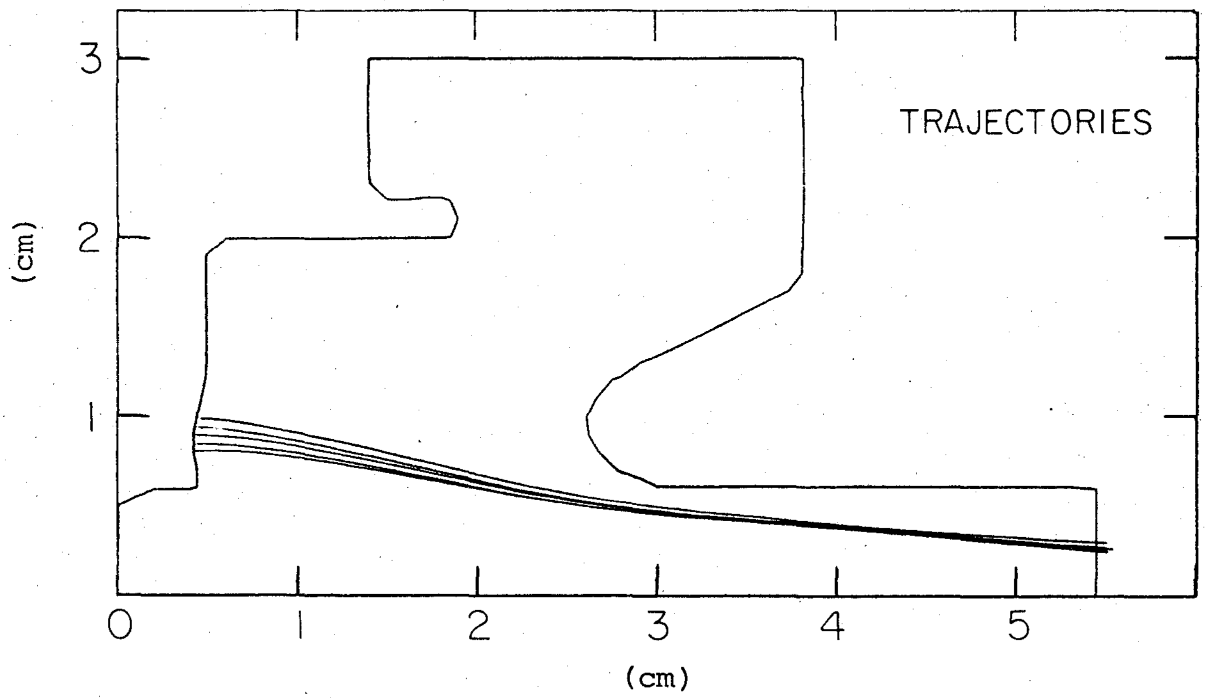

Fig. 3. Electron trajectories in a gun configuration approximating the desired accelerator input optics.

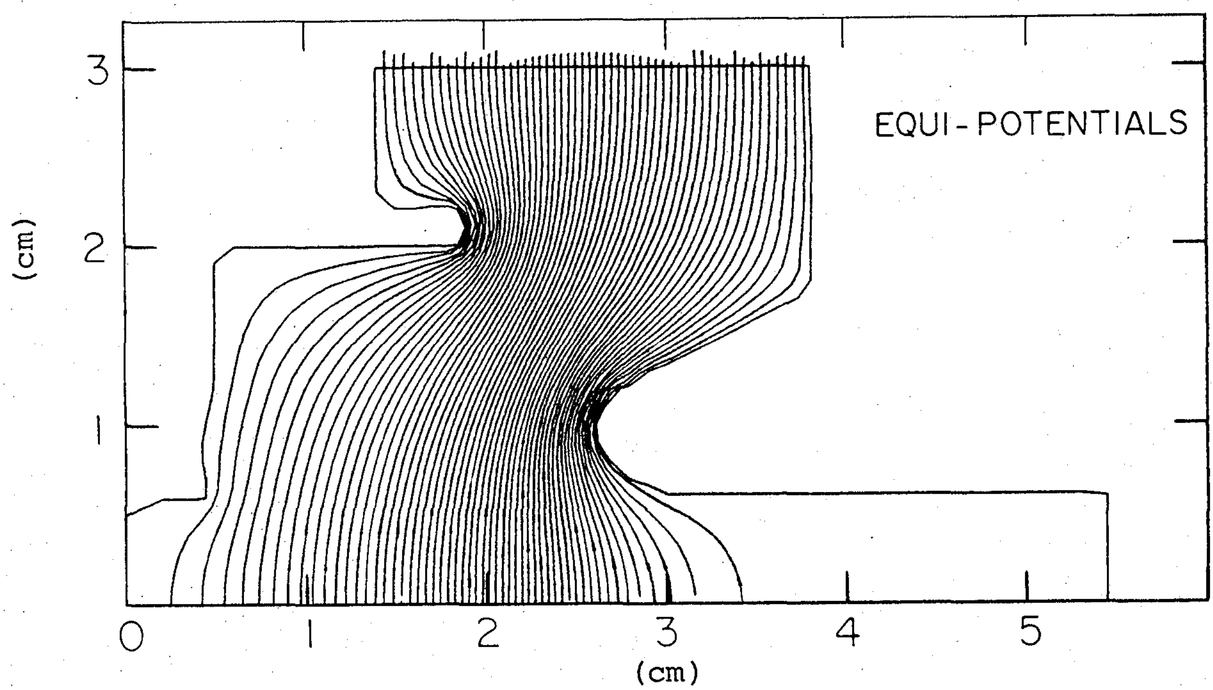

Fig. 4. Equipotential lines for the above gun configuration.

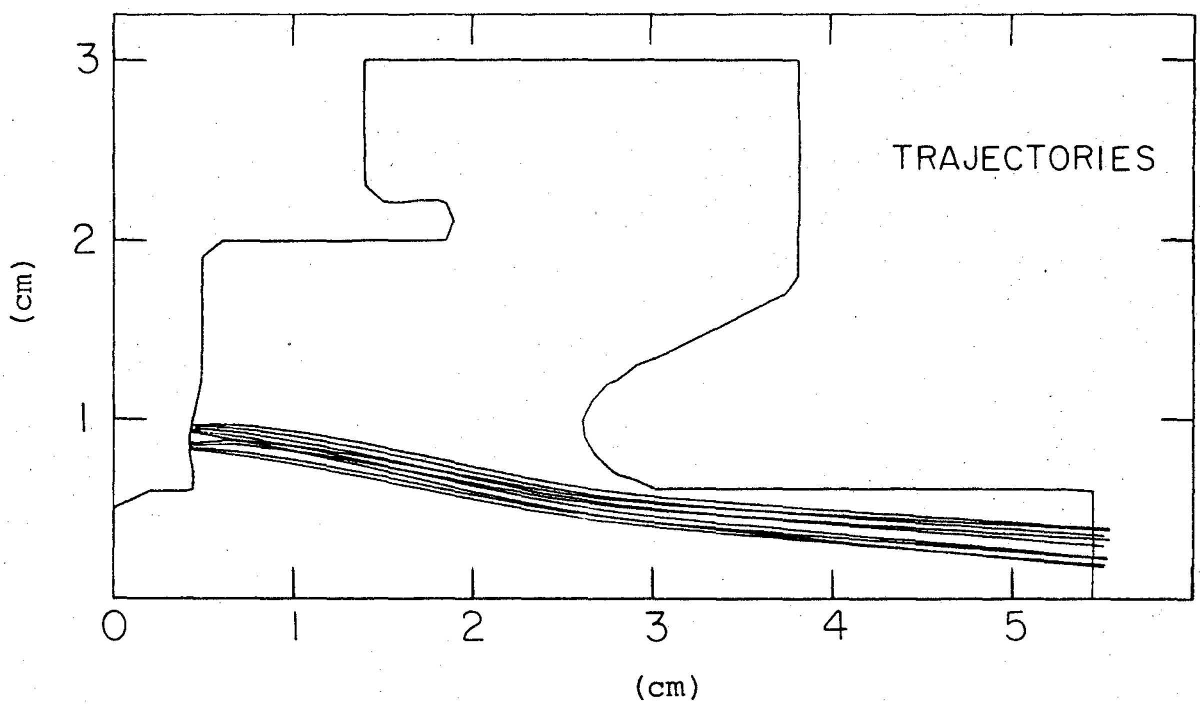

Fig. 5. Electron trajectories calculated for an annular bifilar emitting filament in the same configuration as figure 3.

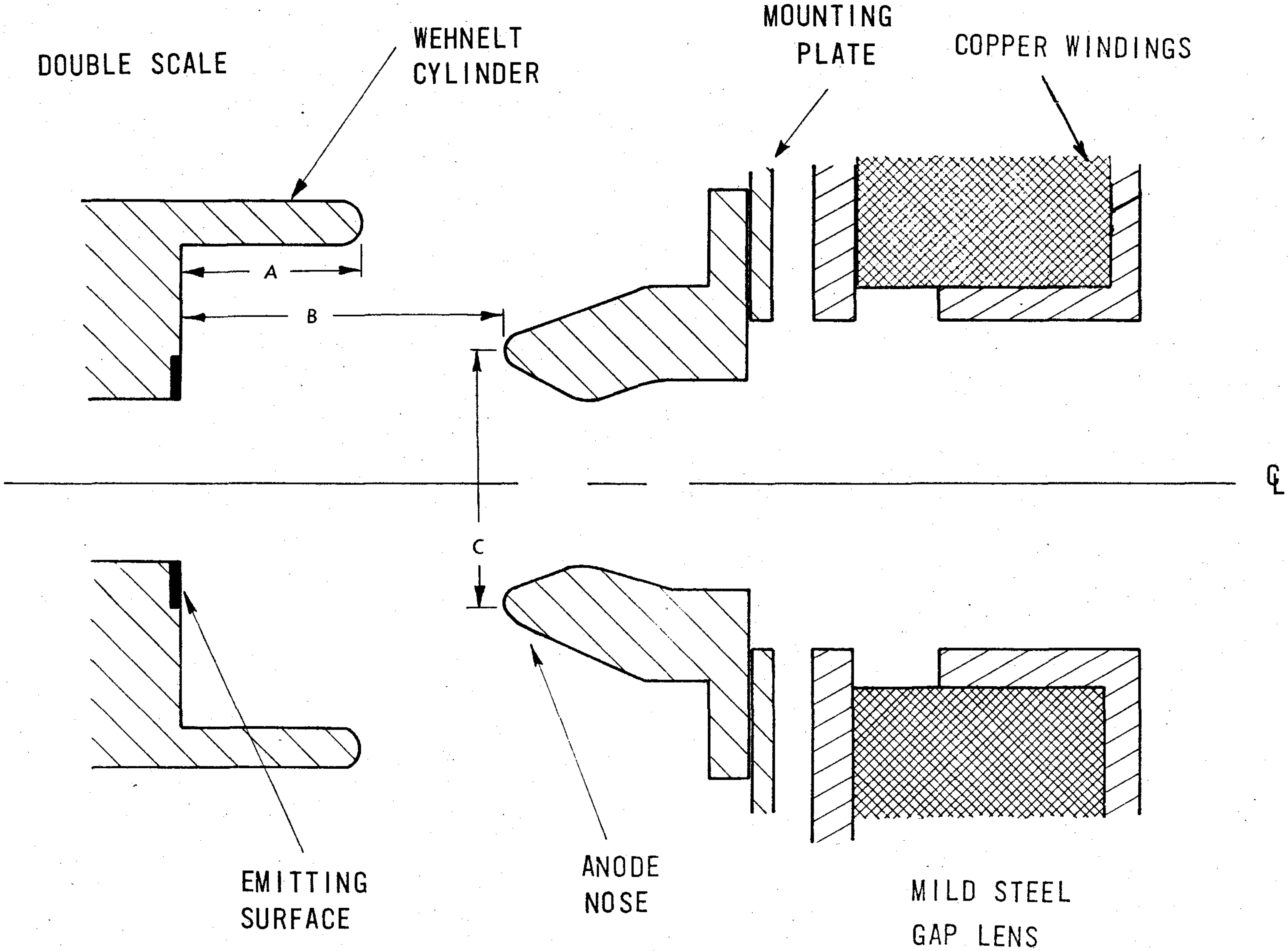

Fig. 6. Cross-sectional view of test electron gun and focus coil.

2.3 Cathode and Anode Shape

The anode and wehnelt shapes of Figure 6 were chosen for the flat ring emitter tests based on information from the computer simulations and CRNL experience with previous guns. The wehnelt diameter and length were preserved from former gun trials in order to use as much of the information as possible for comparison of optics. Thus the outer diameter of the cathode was constrained to be 4.4 cm.

3. MECHANICAL GUN DESIGN

The same geometry was used for both the thoriated tungsten and dispenser cathode emitter guns so that the optics could be compared, and the cathodes could be mounted on the same support structure saving machining time. The prototype accelerator is to operate at three different currents, the maximum required from the gun being 400 mA. To allow for losses and some surface poisoning, the emitter area was chosen to give at least 800 mA at a temperature which would allow an acceptable lifetime. The expected currents at normal operating temperature from the guns as finally constructed are shown below. The tests were done to determine the mechanical and thermal properties of the foils using pure tungsten and tantalum since thoriated tungsten was not immediately available.

TABLE 2

	Conservative Emission	Emitter Area	Expected at Op. Temp.	High Temp. Maximum
Dispenser Cathode	1000 mA/cm^2	1.6 cm^2	1.6 A	16 A
Thoriated Tungsten	500 mA/cm^2	3.2 cm^2	1.6 A	6 A
Tungsten	0.3 mA/cm^2	3.2 cm^2	1 mA	100 mA

The cathode assembly was supported by an angle bracket attached to a stainless steel tube (Figure 7). Stainless steel was chosen over copper since it was suspected that copper would poison the cathodes. Recent experiments have

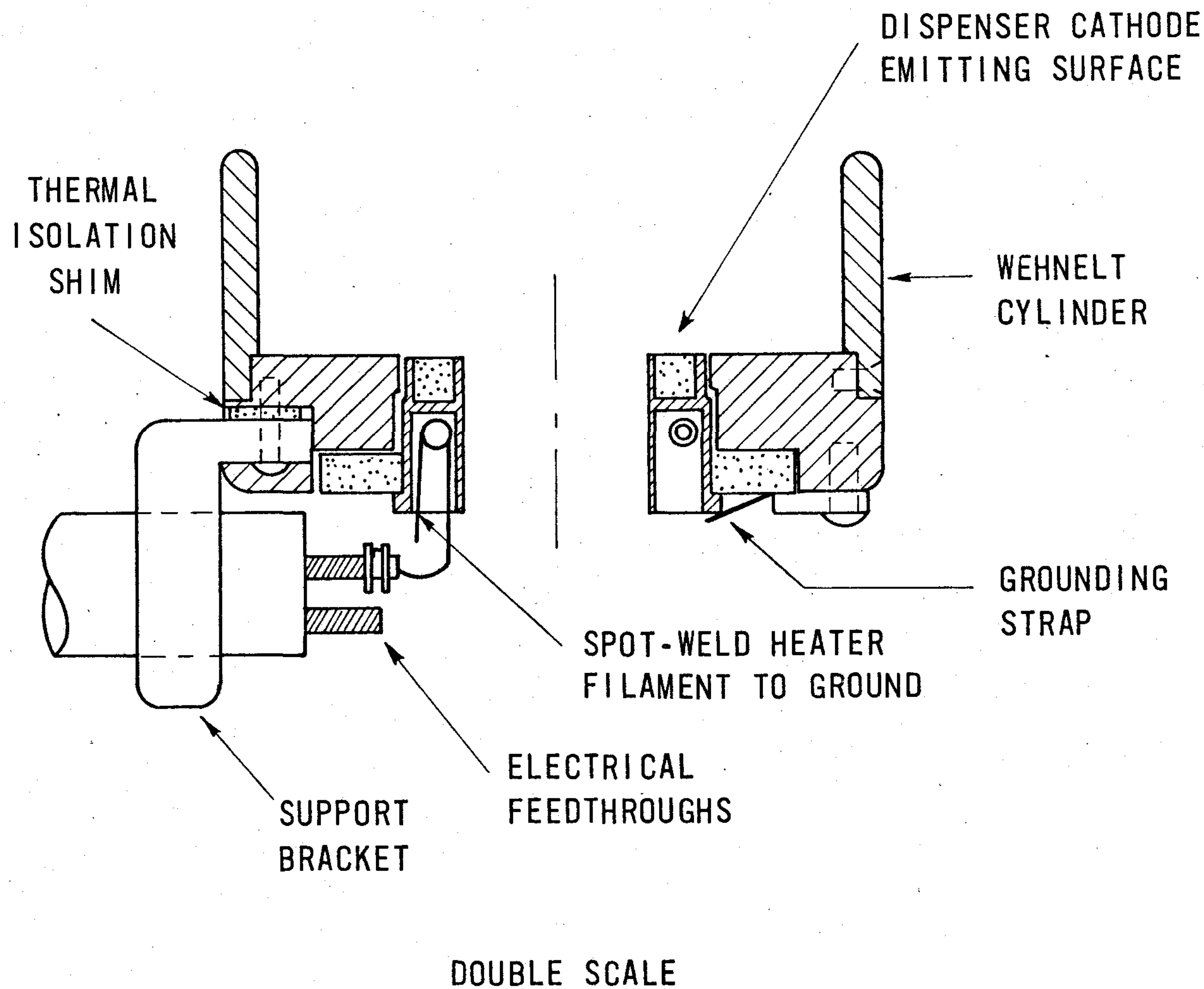

Fig. 7. Detail of dispenser cathode mounting in wehnelt structure.

shown that this is not the case. The 20 cm long rod was sufficiently rigid to hold the cathode firmly although some misalignment was induced as the rod heated and expanded. This problem was eliminated by placing a thermal barrier between the cathode and support rod. The change in length of either type of rod at an average temperature of 200°C is 0.8 mm. The thermal conductivity of copper is over eight times that of stainless steel so it will not expand as much. Future designs will probably use copper as a support structure.

The stainless steel anode nose was secured to the mounting plate with three screws for easy replacement. A focusing coil (gap lens) was also attached to the plate (Figure 6, Sec. 4.5).

3.1 Dispenser Cathode

The dispenser cathode was purchased on special order from Philips Metalonics. The emitting surface, reservoir, and heating filament are encased in a Molybdenum can to which a ceramic disk is brazed. This disk is held in a recess in the cathode plate by three screws so that the emitting surface is flush with the cathode face (Figure 7). In subsequent tests the emitting surface was placed slightly below the cathode face to improve optics. The cathode and wehnelt are both stainless steel to avoid the possible poisoning effects of certain metals[8].

The two cathodes initially tested were difficult to activate and emitted only at very high temperatures. The ceramic to metal braze also cracked allowing the emitter to shift relative to the cathode. It was found that a good electrical conducting path did not exist to the emitting surface so a grounding strap was placed between the molybdenum can and the stainless steel body. At the same time the entire cathode assembly was thermally isolated by placing a 0.64 mm thick sheet of alumina between it and the mounting bracket.

Electrical contact was maintained by two screws.

The third cathode tested with the above modifications activated in less than two hours. 1.5 A was emitted at 980°C as opposed to 1.25 A at 1115°C for the unaltered cathode.

3.2 Foil Cathode

There are several technical problems associated with the use of a metal foil ring as an emitter. The foil must be heated uniformly and cannot buckle excessively when hot. The foil must also be attached firmly to the main cathode body.

Figure 8 shows a 0.013 cm thick tungsten foil ring set between an inner and outer cylinder which are separated by a split ceramic ring. The ceramic is secured with screws and current flows radially to heat the foil directly.

It was decided that an electron beam weld of the foil to the base pieces would be the most suitable method to make good electrical and mechanical contact. Electron beam welding was chosen since it is virtually the only means of welding thin and thick pieces together. Since the foil is in good thermal contact with the cathode structure, the latter is again isolated from the support bracket to decrease power dissipation. The cathode components are made of molybdenum since it welds easily to tungsten and has good vacuum properties under ion bombardment and heat.

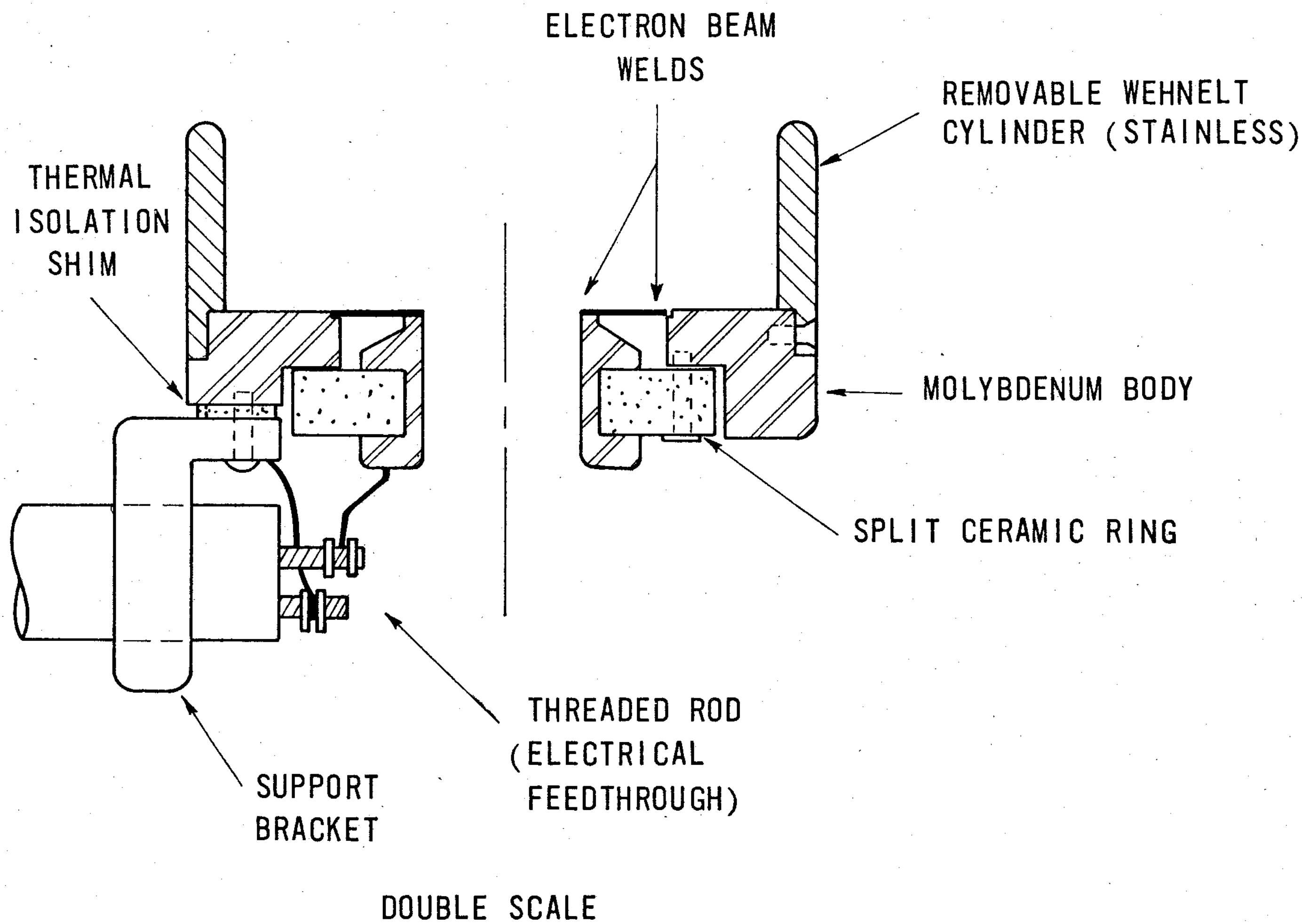

Fig. 8. Detail of proposed emitting foil cathode assembly.

4. TEST APPARATUS

The electron gun test stand is shown schematically in Figure 9. The cathode is pulsed to -42 kV with respect to ground and liberated electrons are accelerated through the anode aperature. A focus coil close to the anode produces a beam focus at the desired point. The beam is observed with a series of nine moveable probes.

A high quality glazed alumina insulator mounted on a vacuum flange served both as a mechanical support for the cathode and as a stand-off for the high voltage. The vacuum chamber, made of 15 cm diameter stainless steel pipe, is mounted directly on the throat of an ion pump for maximum pumping speed.

The test stand is contained in a separate shielded room which is interlocked so that HV can not be applied to the gun unless the entrance door is locked. Consequently all observations had to be made from outside the room and equipment inside had to be controlled remotely.

4.1 Pulsed High Voltage Supply

Figure 10 is a schematic diagram of the high voltage equipment. An RCAF model FPS-507 modulator supplied 4 μsec negative voltage pulses variable between 9.5 and 14 kV. The output impedance was 20 ohms with a pulse repetition frequency (PRF) of 0 - 300 pulses per second (PPS). This high current modulator was used so that it was possible to test the gun and stand-off while approximating accelerator operation. The modulator output pulses were transmitted into the shielded room via paired 50 ohm RG-17 coaxial cable to a 3.1:1 pulse transformer having dual primaries and secondaries wired as shown.

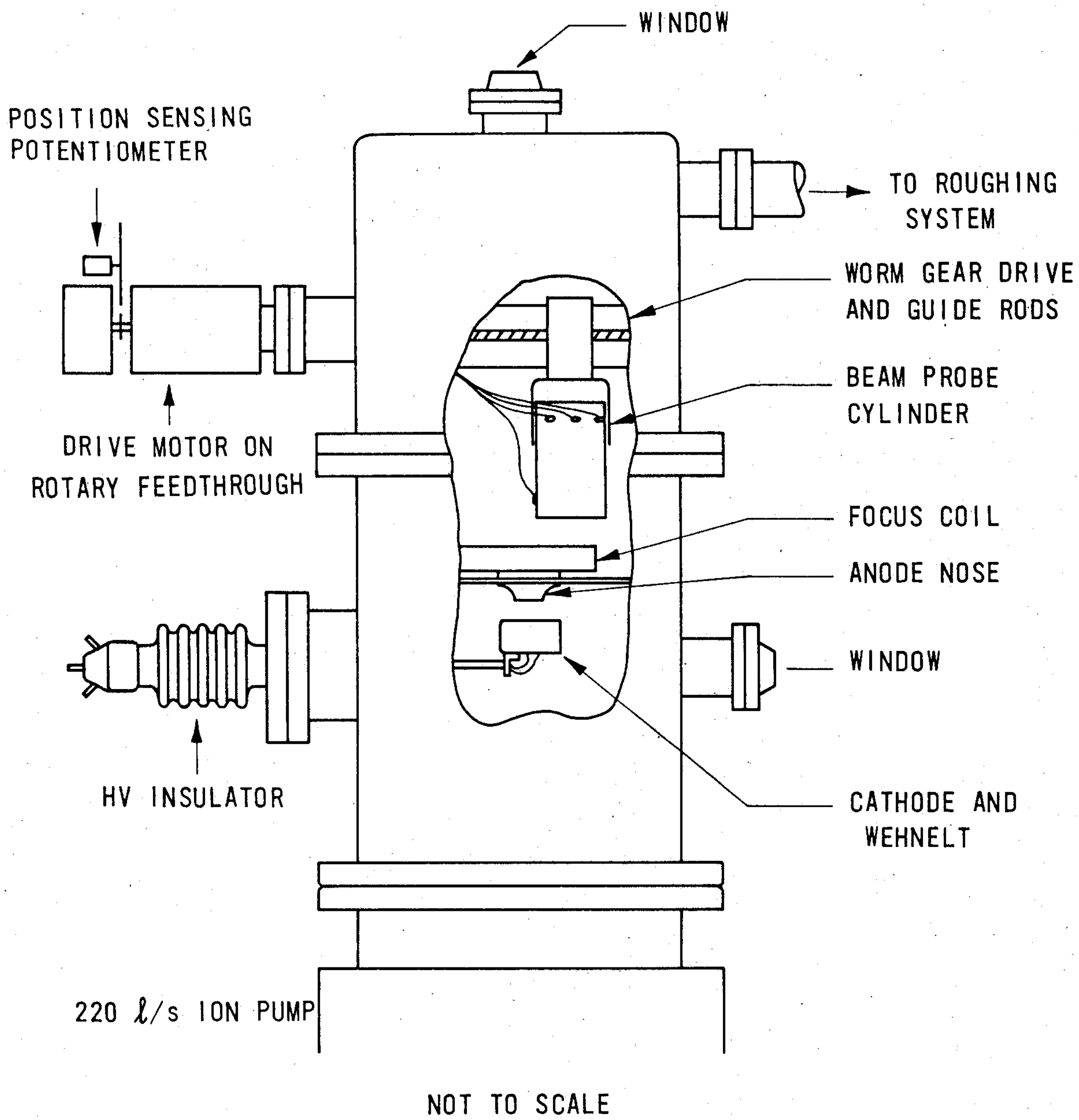

Fig. 9. Cut-away view of annular gun test stand.

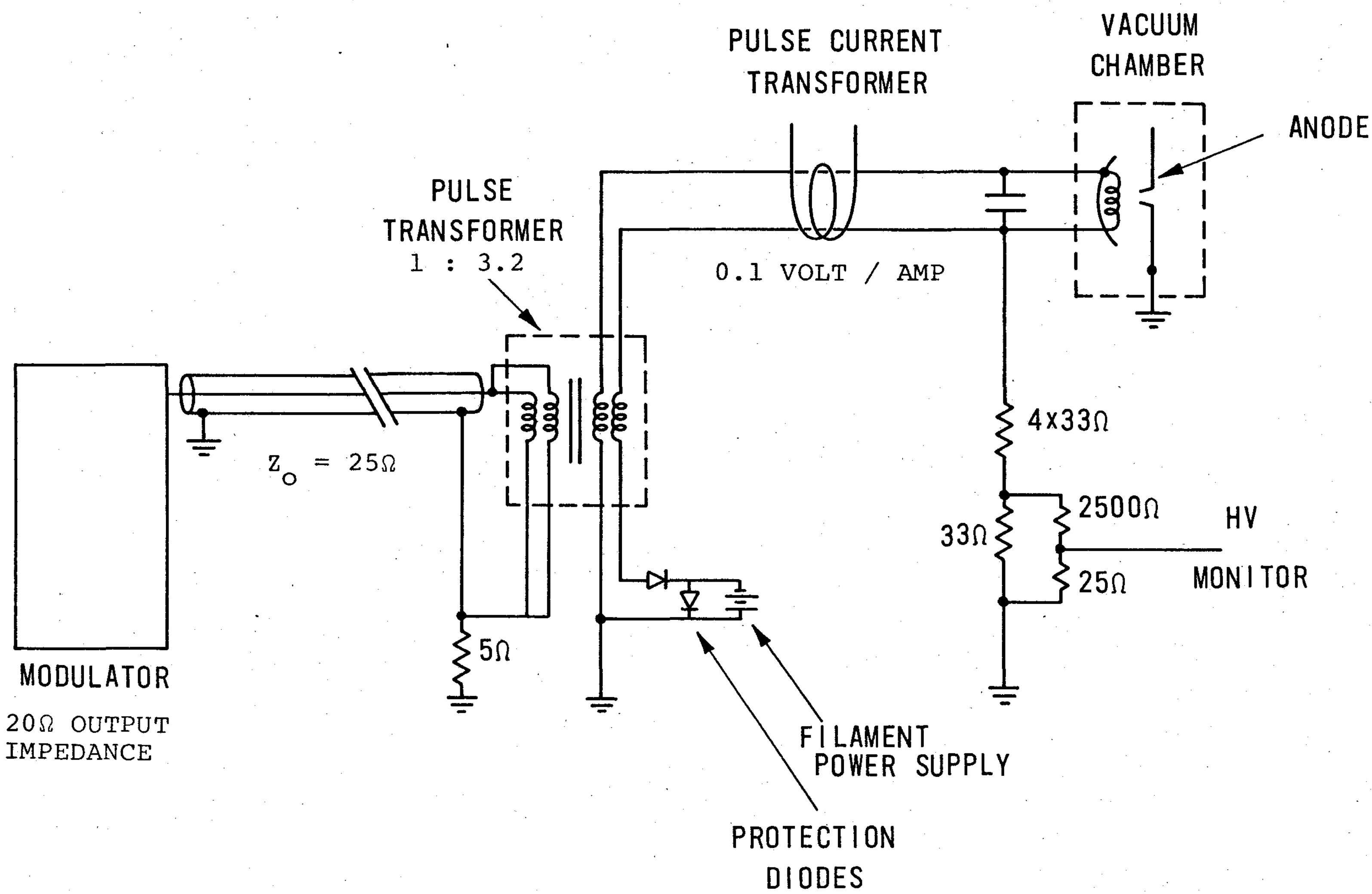

Fig. 10. Schematic of pulsed high voltage network.

The output impedance of the transformer is rated at 220 ohms. A resistive load to ground was wired in parallel with the gun to absorb most of the power and to match the pulse transformer to the very high impedance presented by the gun. The load was experimentally chosen to be five thirty three ohm resistor mat sets in series. For this arrangement the secondary voltage was closest to the modulator output times the pulse transformer turns ratio implying proper impedance matching.

The output end of the coaxial transmission cable was tied to ground through a five ohm power resistor. This resistance was chosen experimentally to minimize pulse "ringing" without creating electronic noise by surging large currents through the building ground system. Some ringing can be observed in Figure 11.

A 1000:1 resistor divider network was wired across the mat at lowest potential to monitor the output pulse. The total resistance was 2500 Ω which allowed sufficient current to flow to minimize capacitive effects. The output pulse shape was improved substantially by locating hook up wires so as to keep ground loops small.

4.2 High Voltage Feedthrough

High voltage stand-offs of various designs have been used on test guns constructed to date but both the insulator and mounting flange sizes were too large for a prototype accelerator. It was decided to test a smaller feedthrough, rated at design voltage, that could be put on a 4 1/2" diameter conflat flange. In the past only two electrical connections had been made to the gun through the stand-off. Anticipating possible future need it was decided to add a third electrical terminal to the feedthrough design.

An Alberox insulator rated at 40 kV was modified as shown in Figure 12. A standard threaded end-cap was

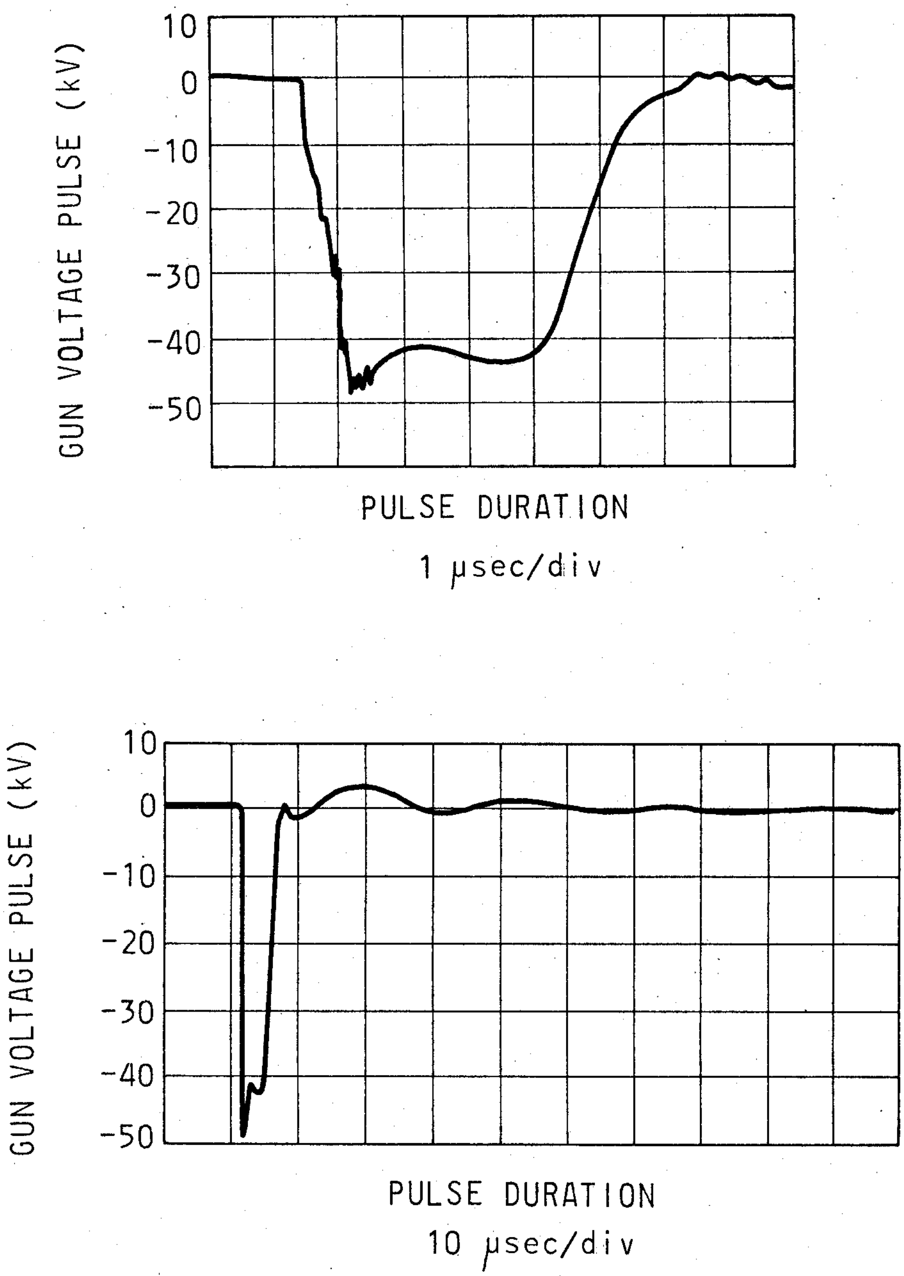

Fig. 11. High voltage pulse applied to the gun as measured by the resistor divider network.

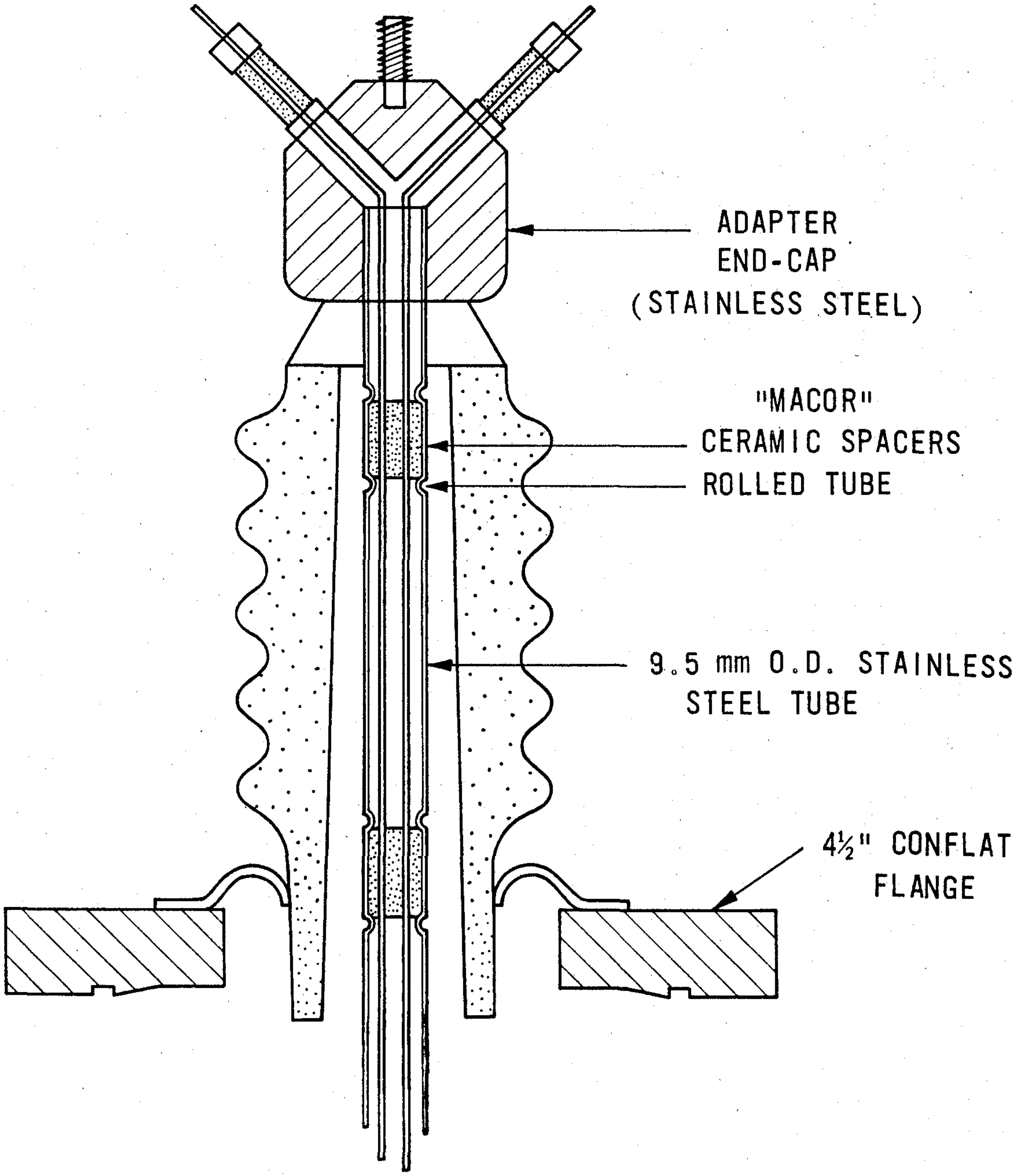

Fig. 12. Cross-sectional view of high voltage insulator and support tube.

removed and replaced with an end-cap modified for two additional electrical inputs. A 0.95 cm diameter stainless steel tube on which the gun was to be mounted was brazed into the end fitting. Two commercially available 0.68 cm diameter feedthroughs were brazed with Cusil alloy at 793°C into the stainless steel end-cap which in turn was brazed to the reworked insulator. The assembly was then welded to a 4 1/2" conflat flange for mounting on the vacuum system.

4.3 Vacuum Chamber

The vacuum chamber (Figure 9) was roughed out with mechanical and sorption pumps to start the 220 ℓ/s triode pump. The system was baked out using heating tapes each time the system was cycled. Base pressures in the range 3 - 10 x 10^{-7} P were achieved after two days pumping.

Using length-diameter conductance curves from Guthrie[22], the conductance between the gun and the ion pump was estimated to be 280 ℓ/s. The pressure drop is the mass flow rate divided by the conductance. With the effective pump speed determined from the manufacturer's specifications the cathode pressure was found to be twice the observed ion pump pressure.

Two clear untinted windows made it possible to take optical pyrometer readings of emitter temperature and also gave visual confirmation that the appartus was functioning correctly.

4.4 Beam Diagnostics

Beam current was measured in two ways: a current sensing toroid measured total emitted current and a set of moveable beam probes scanned the beam to get profiles.

A "pulse current transformer" or current sensing toroid was placed on the filament supply lines between the pulse transformer and the high voltage stand-off (Figure 10).

Rated at 0.1 V/A, it measured the net current flow through the wires or the current emitted from the cathode.

A set of small "Faraday cups" made of 3 mm square copper foil was arranged within a stainless steel cylinder to detect the beam current at nine spatial locations (Figures 13 and 14). If the beam direction is referred to as the z axis with z = 0 at the emitter then three squares were located at each of three z values, z = 9, 12, and 15 cm.

The probe assembly was secured to a mild steel block which slid on two guide rods. The unit could be translated from side to side by rotating a worm gear which drove a ballnut in the sliding block. A stepping motor supplied the torque and the position of the probes was sensed with a ten turn 100 kΩ potentiometer. The guide rods were made of mild steel and it was found that the steel on steel sliding contact would seize after some use in vacuum. The problem was resolved by inserting brass sleeves in the support block.

Spatially separated probes, when hit with an electron beam can interact in two ways. Electrons transmitted through one probe may be collected by a downstream probe, or secondary electrons can induce spurious pick-up in probes which are upstream of the one being considered. For probes to be useful such cross-talk must at most be a small fraction of the total signal.

The range for 30 kV electrons in copper is 4.7 x 10^{-3} g/cm^2 or roughly 6 μm[23]. Since the probes were more than 100 μm thick all electrons were stopped and counted except for a small fraction hitting within 6 μm of the edge of the probes. These could undergo small angle collisions and still be transmitted. They must therefore be considered further. The ratio of the area of the outer 6 μm wide band to the area of the inner mutually exclusive square is 10^{-2}. Assuming the worst condition - that no electrons are absorbed in the band - the solid angle subtended by a probe downstream

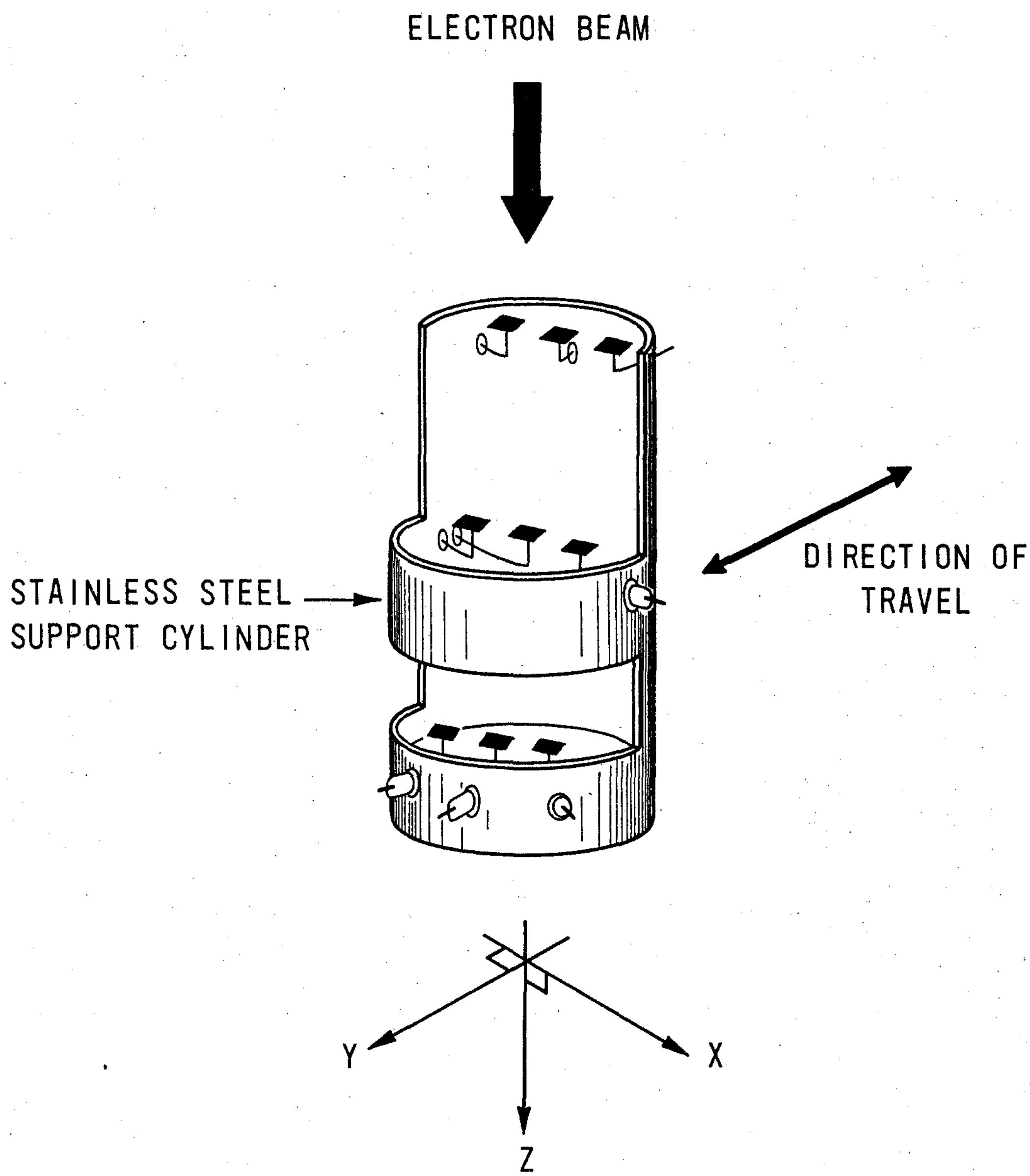

Fig. 13. Pictorial view of intercepting copper beam probes.

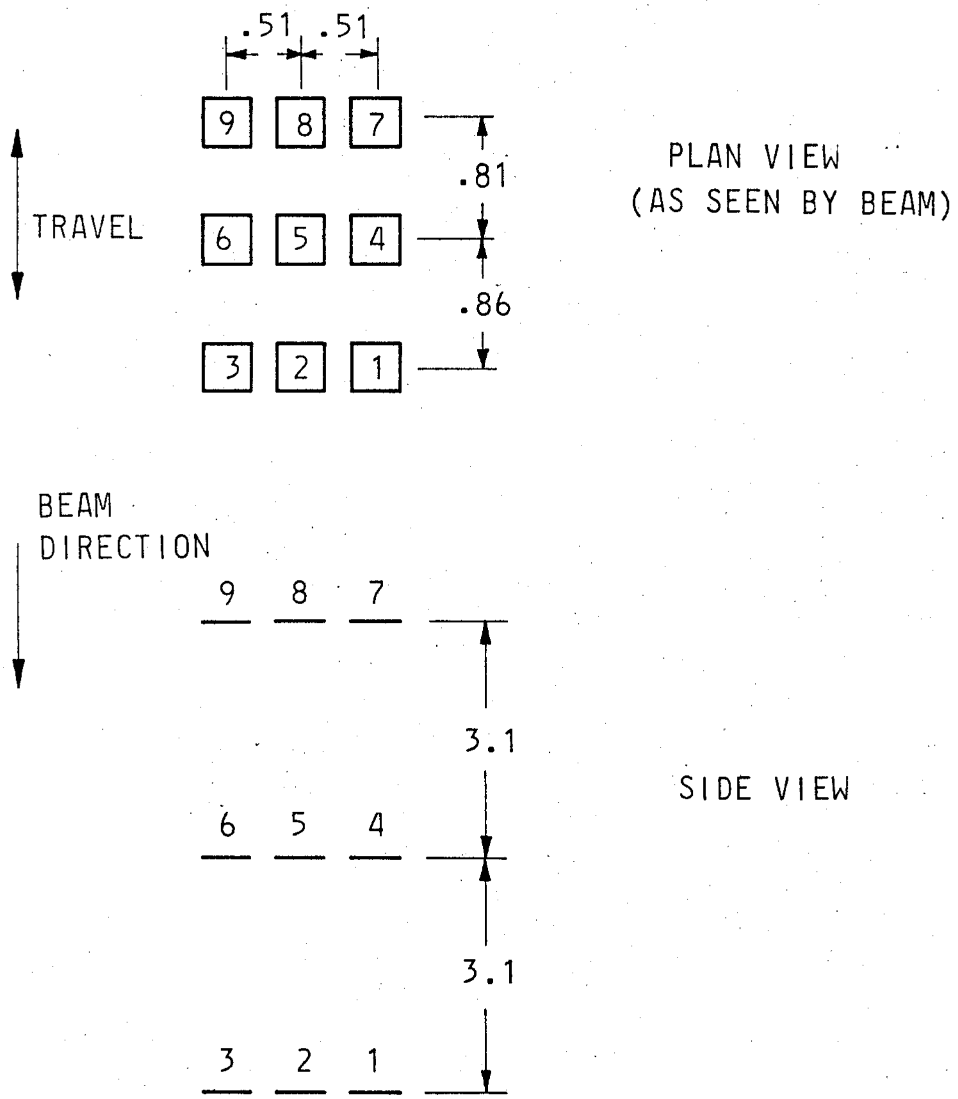

Fig. 14. Schematic view of intercepting probe geometry. Individual probes will subsequently be referred to using the label numbers shown.

is no larger than 10^{-2} of possible scattered solid angle. The net cross-talk from transmission effects is no more than 10^{-4} of the incident current and so is not taken into account in the analysis.

Approximately 30% of the incident beam intensity will be given off as secondary electrons[24]. From the previous solid angle argument, an upstream probe will only see 1% of these secondaries. Even neglecting the angular dependence of the secondaries, the maximum cross-talk is 0.3% which is also negligible.

More importantly, the previous reference shows that only 70% of the beam will be detected since 30% of the incident charge leaves as secondaries. Also scattering from the stainless steel walls and the cylinder mounting block will give an unwanted background current so portions of the cylinder were removed to minimize this effect. Pick up on the mounting wires must also be considered. The area of exposed wire is small compared to the probe area, and in cases where pick-up from the support wire is significant, the probe scan shows extra information which can easily be rationalized.

4.5 Focus Coil

The focus coil was made of 150 turns of polyimide coated #16 copper wire wound in a mild steel (1020) housing with a gap of 0.635 cm and a beam hole diameter of 2.54 cm. From Septier[25], the focal length for a magnetic lens of aperture diameter D and gap width S is calculated using the following defined quantities:

$$f_{1M} = 0.5 \left[S^2 + 0.45\, D^2 \right]^{1/2}$$

$$NI_o = 13.5\, (V^*)^{1/2} \text{ where } V^* = V \left(1 + \frac{|qV|}{2m_o c^2} \right)$$

where q and m_o are the charge and mass of an electron and c is the speed of light. For the present case, $f_{1M} = 1.02$ cm and $NI_o = 2.99 \times 10^3$ at 42 kV.

The focal length is then given by

$$f = \frac{0.897\, f_{1M}}{\left(\frac{NI}{NI_o}\right) \sin\left(2.029\, \frac{NI}{NI_o}\right)} .$$

With N = 150 turns, then for I = 6A, f = 5.3 cm and for I = 3A, f = 20.3 cm.

Since the coil was mounted inside the vacuum chamber, special precautions were required. The windings were baked in air at 200°C for two hours after chemical washing. The current was only turned on while a measurement was being made so that the coil never overheated. No problems were experienced operating the coil at 6A for periods of several minutes.

5. PREPARATIONS, RESULTS AND DISCUSSION

5.1 Preparations

The gun test stand at CRNL was committed to the study of emitting wire filament guns so a second test stand was required for the planar emitting surface gun trials. The room chosen for this had previously been used for experiments on a small electron accelerator, and while many of the interlock and control systems still functioned, others required rewiring and debugging. The control panel was modified so as to interface to an FPS-507 high power radar modulator. Many interlocks were no longer required so these were bypassed at the designated jumper box.

The individual modulator units (high voltage supply, power transformer, regulator chassis, pulse forming network) were interconnected, the 208 V 3Ø power was wired in, and the control system connected. The high voltage cable was run to the pulse transformer in the shielded room and the system was made operational.

While the vacuum chamber was being constructed in the mechanical shops, the roughing system and the probe housing drive mechanism were being assembled. The stepping motor on the probe drive required a control and power box so that the speed could be varied and the direction of travel reversed. Supporting electronics such as ion pump controller, current supplies, chart recorder, X-Y plotter, modulator trigger and oscilloscope were also wired in. The total installation of the electron gun test facility took two and one half months to complete.

5.2 Disperser Cathode

5.2.1 Geometry and Operation

The dimensions which essentially determine the gun optics (Table 3) were taken from the optimum computer case (Figure 3) and were used for the test gun #1. The letters (A, B, C) on Table 3 refer to the dimensions so labelled in Figure 6.

TABLE 3

	Dimension	(cm)
A	Wehnelt length	1.40
B	Tip of anode nose to cathode face	2.54
C	Anode hole diameter	1.91

In preliminary runs it appeared that some of the beam was hitting the anode nose. To improve the transmission, the emitting surface was recessed 0.06 cm below the cathode face as indicated by computer plots where such a change caused the beam to converge more rapidly.

The dispenser cathode was activated by slowly increasing the filament current while maintaining the pressure at the gun below 5×10^{-4} P. The emitting surface temperature as read by optical pyrometer through the clear glass window was 870°C at 9.0 A (filament) and 980°C at 11.0 A (filament). The current was increased until the emitter reached 1150°C at which point the cathode gradually began to emit. Poisoning was not significant for pressure below 5×10^{-5} P and it is probable that the cathode could be operated at higher pressures for short periods without harm. When poisoning did occur, the cathode was reactivated by bringing the filament current up to 12.5 A for approximately one minute.

Figures 15 and 16 show the dispenser cathode emitted current as a function of dissipated power and filament heating current respectively. It is apparent that the cathode is emission limited.

To improve the optics by reducing the convergence angle, gun #2 was constructed with an anode hole diameter of 2.29 cm (20% larger than gun A). A new dispenser cathode was also used since the filament wires on the old one became brittle and broke during handling.

The emitted current versus filament current for un #2 is shown in Figure 17. The difference between this characteristic curve and that of gun #1 could be attributed either to the modified potential gradient at the cathode or to an increased susceptability to poisoning from ions backstreaming through the larger hole. There was insufficient time to study these effects.

5.2.2 Optics

Figures 18 and 19 give the output of the nine current sensing probes as a function of position across the gun #1 beam for zero and 6A focus coil current respectively. The apparent center lines for each group of three probes have been graphically aligned with the center line of the cathode and anode to compensate for the shift of one group relative to another within the mounting cylinder, and to remove small displacements caused by beam misalignment and stearing effects. A slight misalignment is apparent in Figure 18 since probe #6 shows an annular beam while probe #4 sees only the edge. These curves were taken at 42 kV with a PRF = 13 PPS, a filament current of 9.5 A, a total emitted current of 100 mA, and a pressure of $3x10^{-6}$ P.

Since the $(3\ mm)^2$ probe size is folded into the resultes a deconvolution is required to extract the true beam dimension. Since the curves are roughly triangular, a

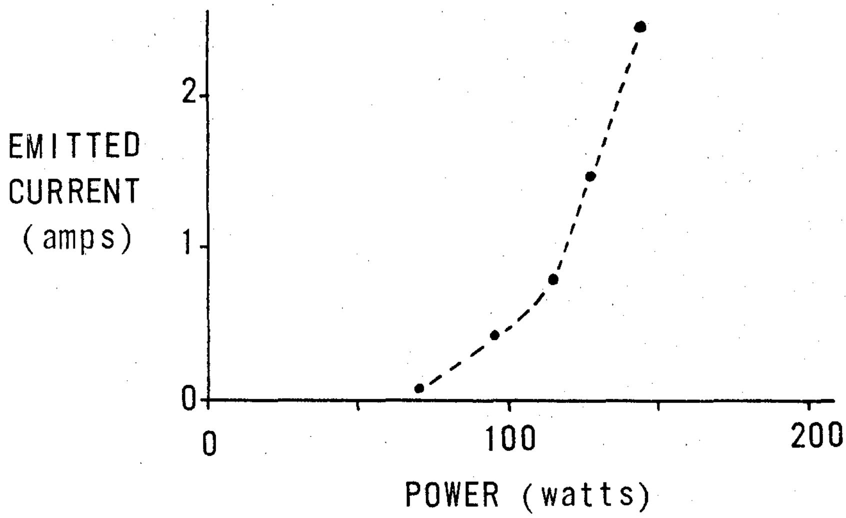

Fig. 15: Emitted cathode current versus heater power dissipation.

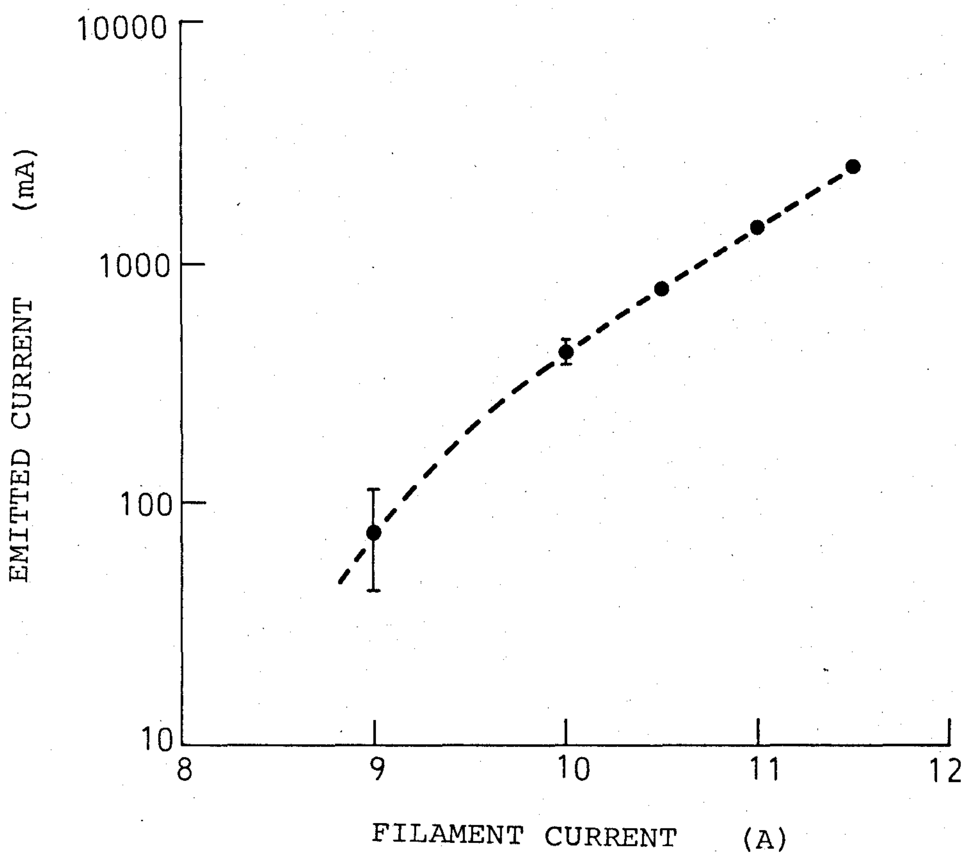

Fig. 16: Emitted cathode current versus header filament furrent for gun #1.

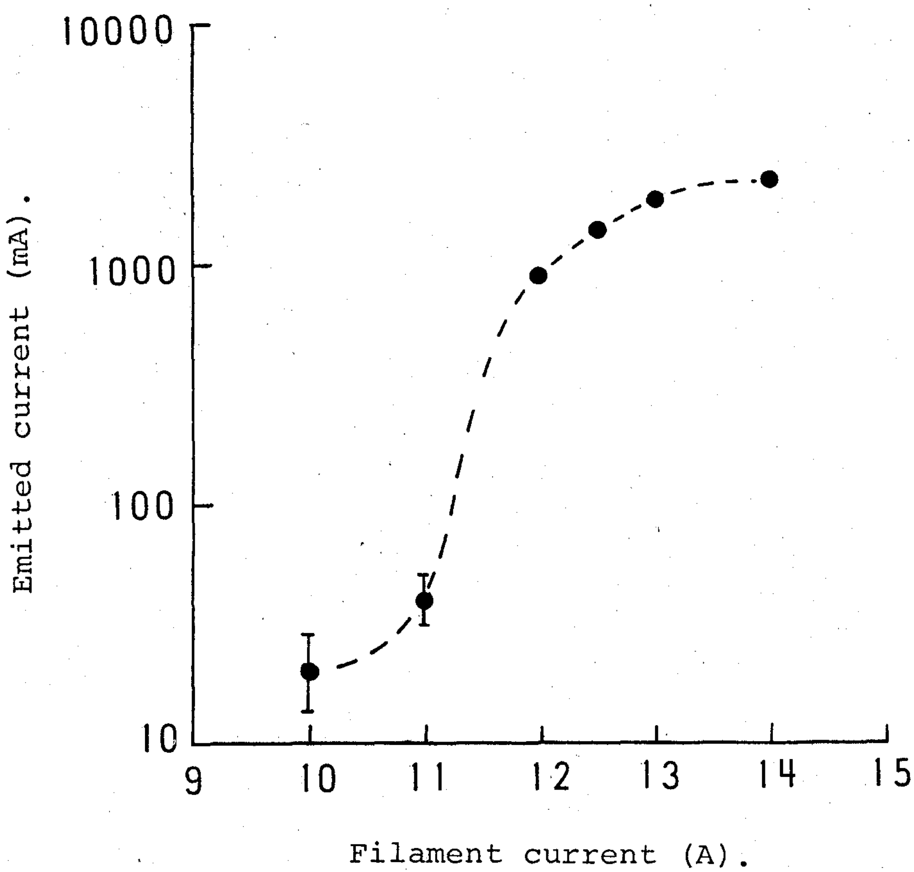

Fig. 17: Emitted cathode current versus header filament current for gun #2.

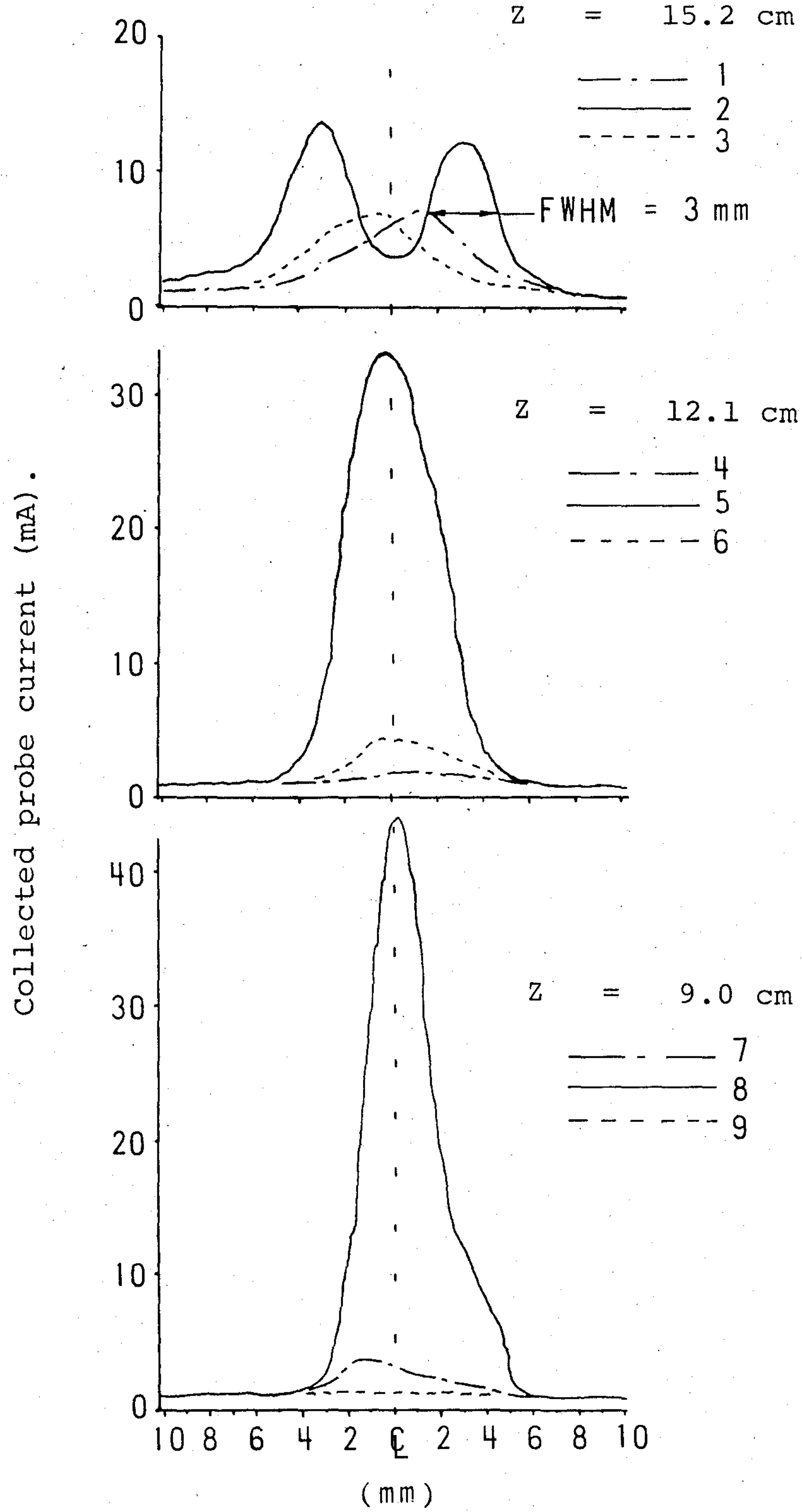

Fig. 18: Current collected on respective beam probes (labelled 1 through 9) during a lateral sweep through the beam. See Figure 14 for specific probe geometry. No focus coil current.

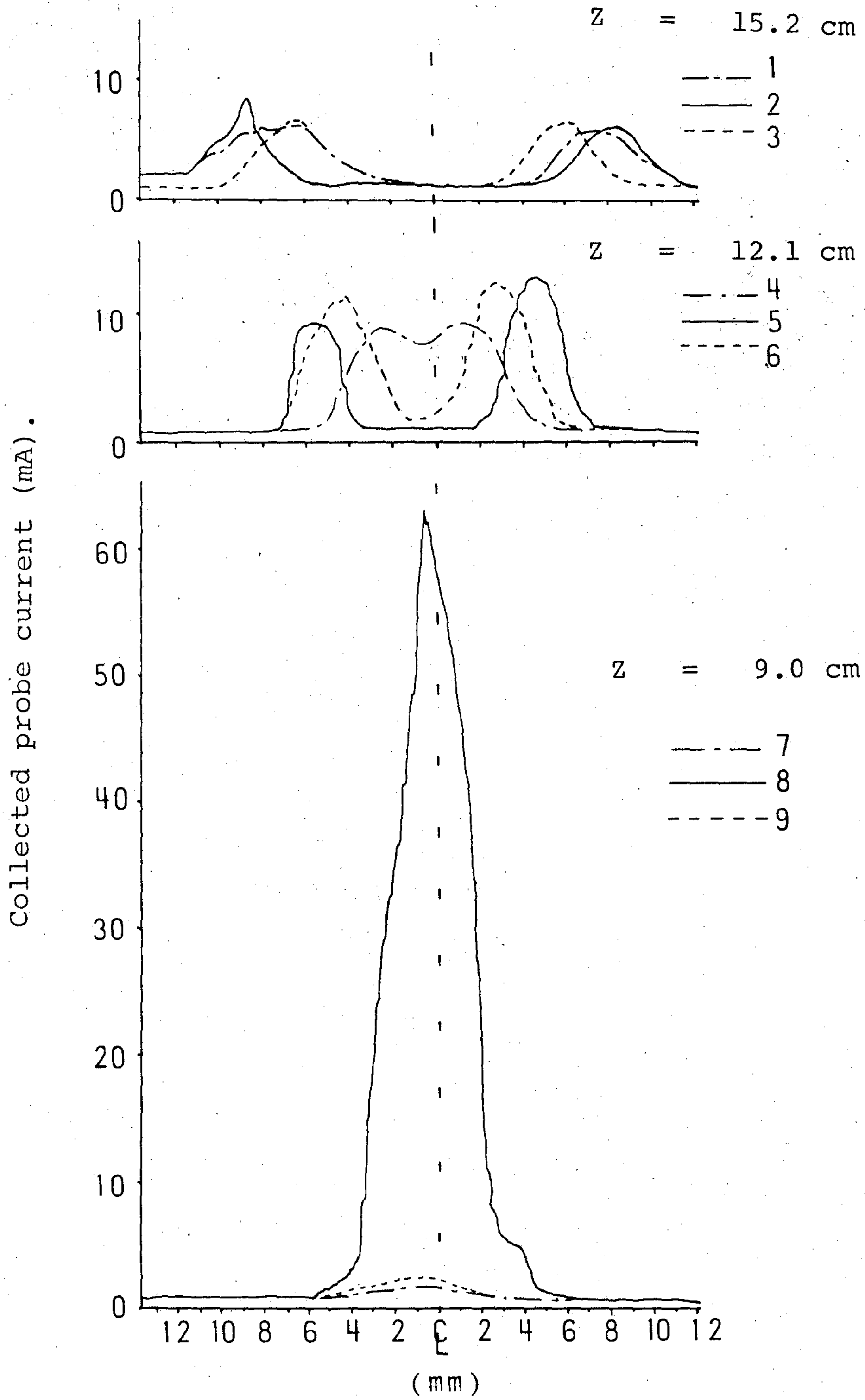

Fig. 19: Current collected on respective beam probes (labelled 1 through 9) during a lateral sweep through the beam. See Figure 14 for specific geometry. Focus coil current = 6A.

simple analysis indicates that the beam annulus must have very well defined inner and outer edges and a fairly uniform density cross-section. The overlap (or convolution) of two gate functions, approximating the beam and the probe, has a full width at half maximum (FWHM) equal to the width of the wider function. Therefore, a minimum FWHM of at least 3 mm is expected for all curves, reflecting the probe size. A FWHM larger than this is a measure of the true beam dimension.

The trajectories of Figures 20 and 21 were derived from Figures 18 and 19 with the assumed beam shape and ignoring space charge blow up effects. Calculations showed that the Coulomb induced divergence for beams up to 1A was small, and tests made with emitted currents larger than 1A gave the same optics as the low currents. The trajectories shown are for the largest possible beam divergence and diameter (represented by the arrow heads) and therefore the maximum emittance.

Figures 22 and 23 were obtained for gun #2 following the analysis used previously. At zero focus coil current the beam is so small and nearly parallel that the probe system is at the limit of its resolution. More information about the beam width was obtained from the 3A and 6A focus coil current data where the beam width is comparable with the probe size.

By integrating the intensity profiles and normalizing the result with respect to the total emission (as measured on current sensing toroid) it was found that both guns transmitted the same fraction through the anode hole.

The transmitted current was estimated by considering the profiles for the 6A focus current case. The beam annulus diameter is measured and its width is equal to or less than 3 mm, as previously discussed. Thus the peak current over the profile represents the current

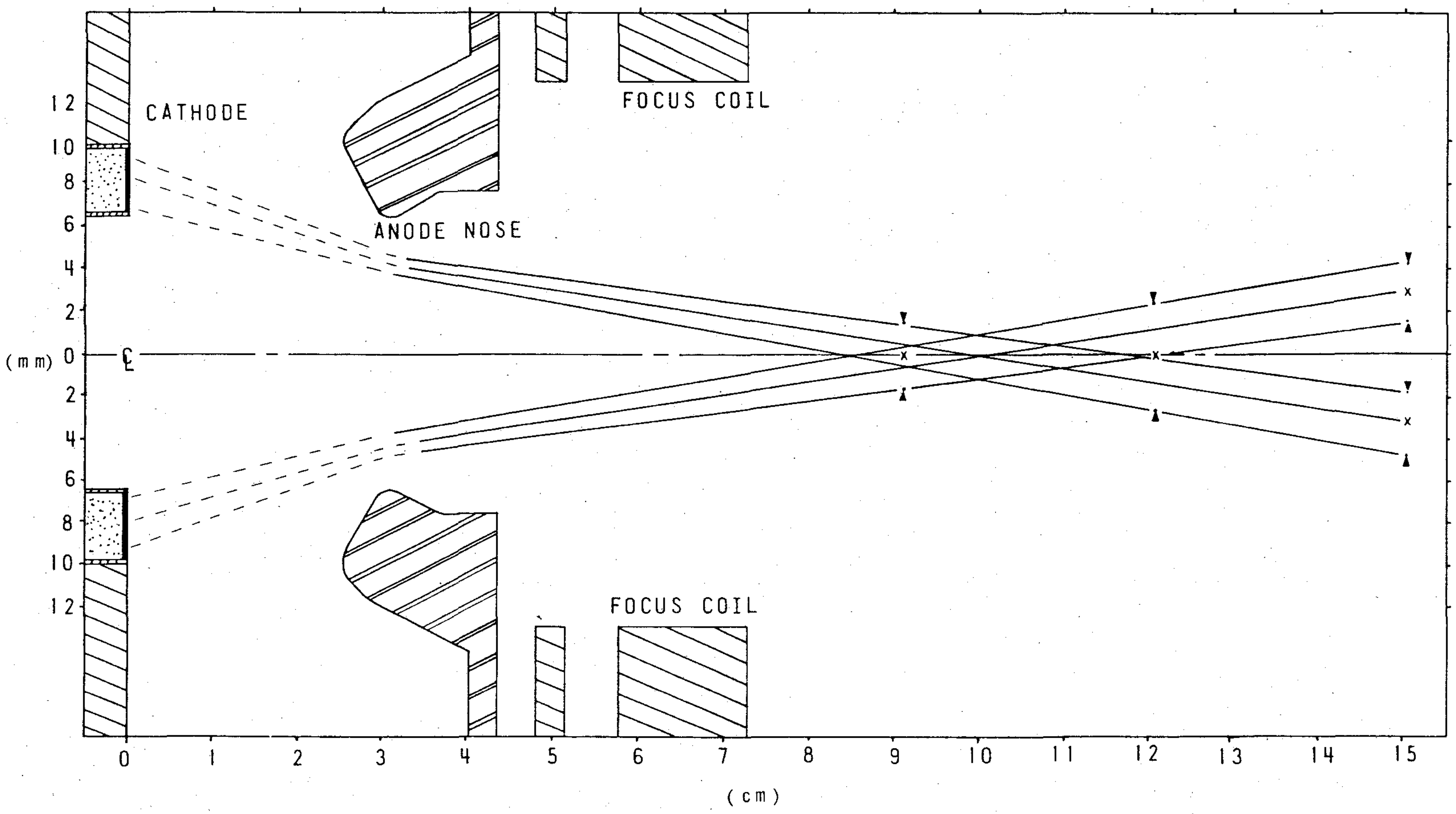

Fig. 20: Schematic representation of gun #1 beam trajectories as deduced from the lateral probe current distributions (Figure 18) for OA focus coil current. The arrow heads represent the maximum possible beam dimensions (see text). Note that the radial scale is expanded by a factor of 2.5. The mean beam convergence angle is 3.6°.

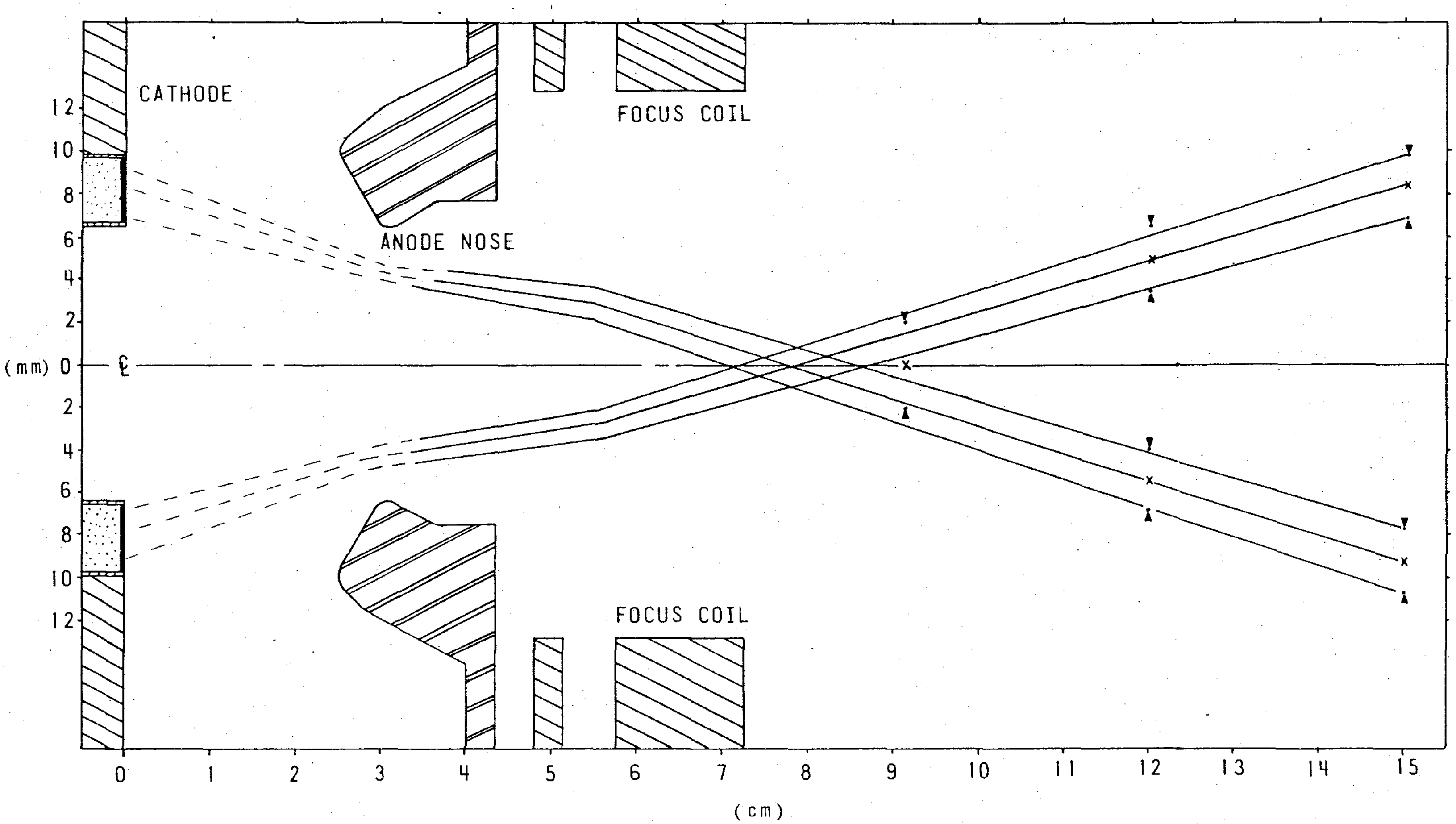

Fig. 21: Schematic representation of gun #1 beam trajectories as deduced from the laterial probe current distributions (Figure 19) for 6A focus coil current. The arrow heads represent the maximum possible beam dimensions (see text). Note that the radial scale is expanded by a factor of 2.5.

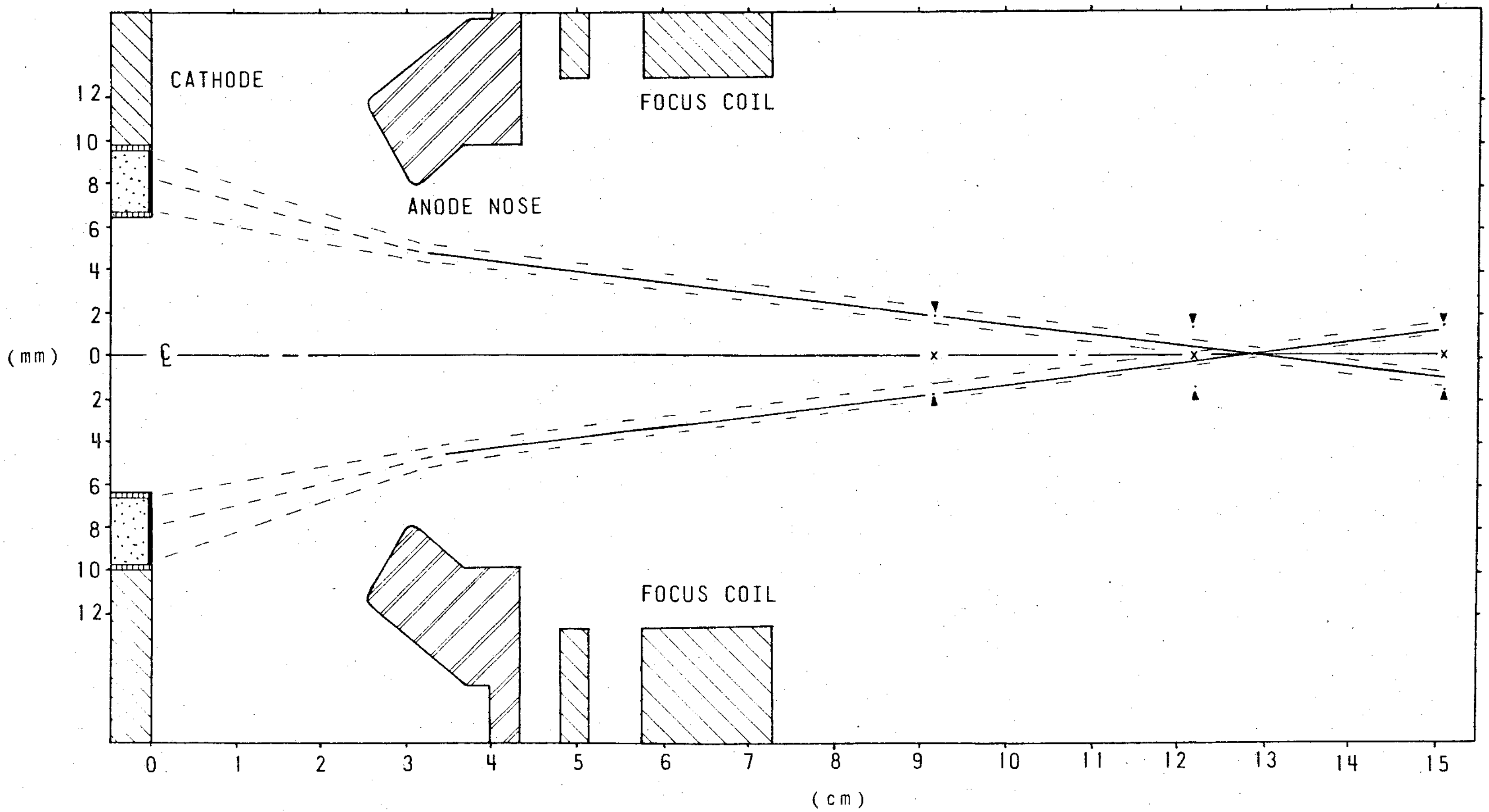

Fig. 22: Schematic representation of gun #2 beam trajectories as deduced from lateral probe current distributions for OA focus coil current. The arrow heads represent the maximum possible beam dimensions (see text). Note that the radial scale is expended by a factor of 2.5. The mean beam convergence angle is 2.8°.

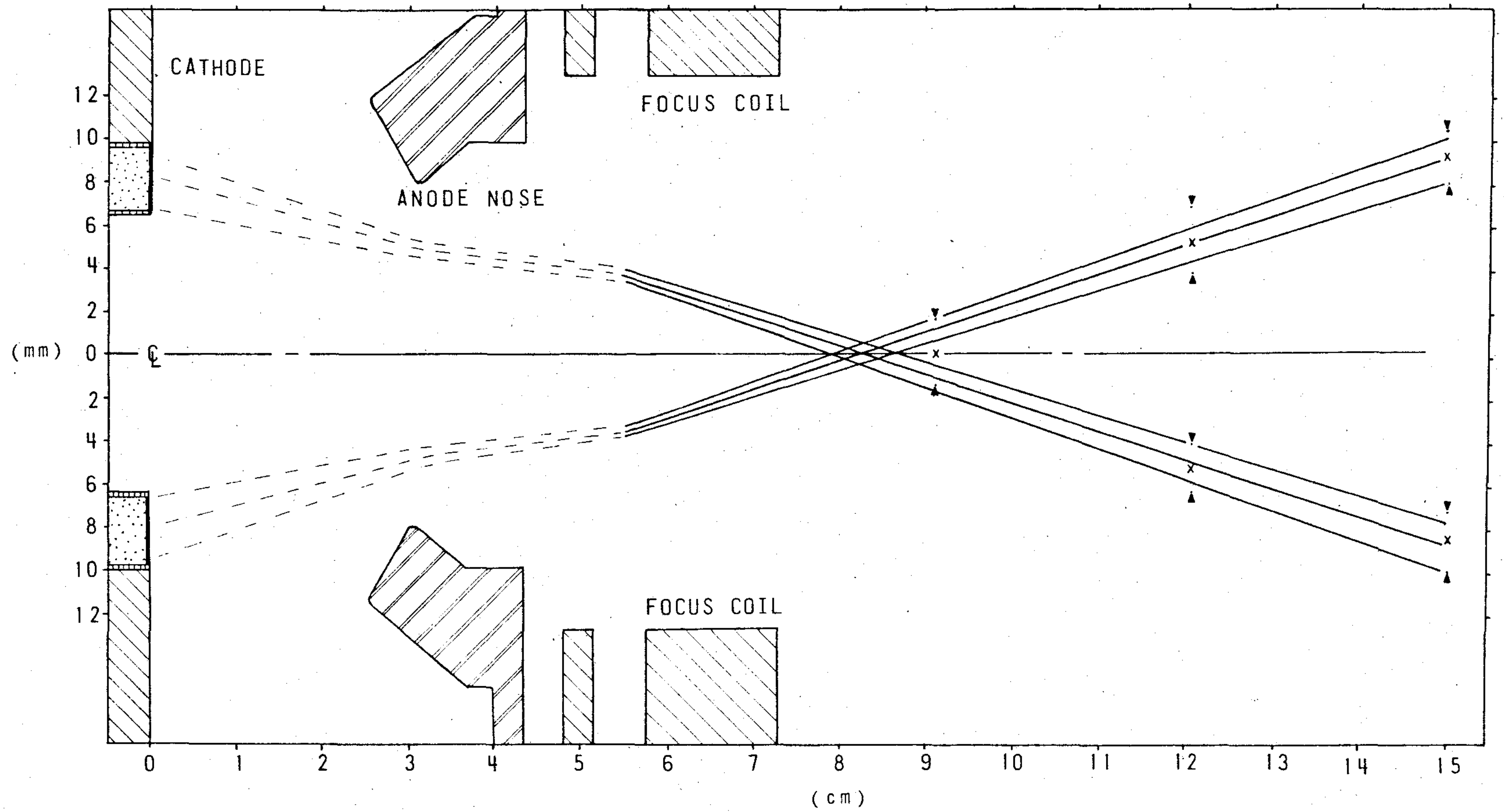

Fig. 23: Schematic representation of gun #2 beam trajectories as deduced from the lateral probe current distributions for 6A focus coil current. The arrow heads represent the maximum possible beam dimensions (see text). Note that the radial scale is expanded by a factor of 2.5.

collected over a 3 mm segment of the bean annulus circumference. Using this method, both guns give total currents of 480 mA ± 2%. When a secondary emission loss of roughly 30% is accounted for, the transmitted current is about 700 mA. The current measured on the toroid was 800 mA ± 30 mA so within the limits of error on the secondary emission coefficient, all of the beam is transmitted through the anode hole for both guns.

The emittance for gun #1 is less than 30 cm mrad, while for gun #2 it is less than 20 cm mrad. With the focus at 13 cm from the emitting surface, and the 2.8^{o} convergence angle, gun #2 approaches the ideal optics for the accelerator without the need of a focusing coil.

5.2.3 Time Response

It is necessary to know how rapidly the gun emission responds to heater current changes to evaluate the effectiveness of dose control systems. The cathode time constant is defined as the time required for the emitted current to change by e (63%) of the difference between initial and final currents, following a small step change of the filament heater current.

Figure 24 gives the time response of the dispenser cathode. The time constant for an increase in heater current is approximately 50 seconds while that for a decrease is greater than 175 seconds and varies somewhat with the size of the perturbation. There is a fine structure apparent on the large positive change. This has not been fully explained but may involve an ion heating feedback mechanism.

It is clear that a done control system cannot rely solely on heater current changes since there is too much thermal inertia. Short term dose adjustments must therefore be made by varying the PRF, which is a less satisfactory method. The situation could be improved by decreasing the amount of material which must be heated. It

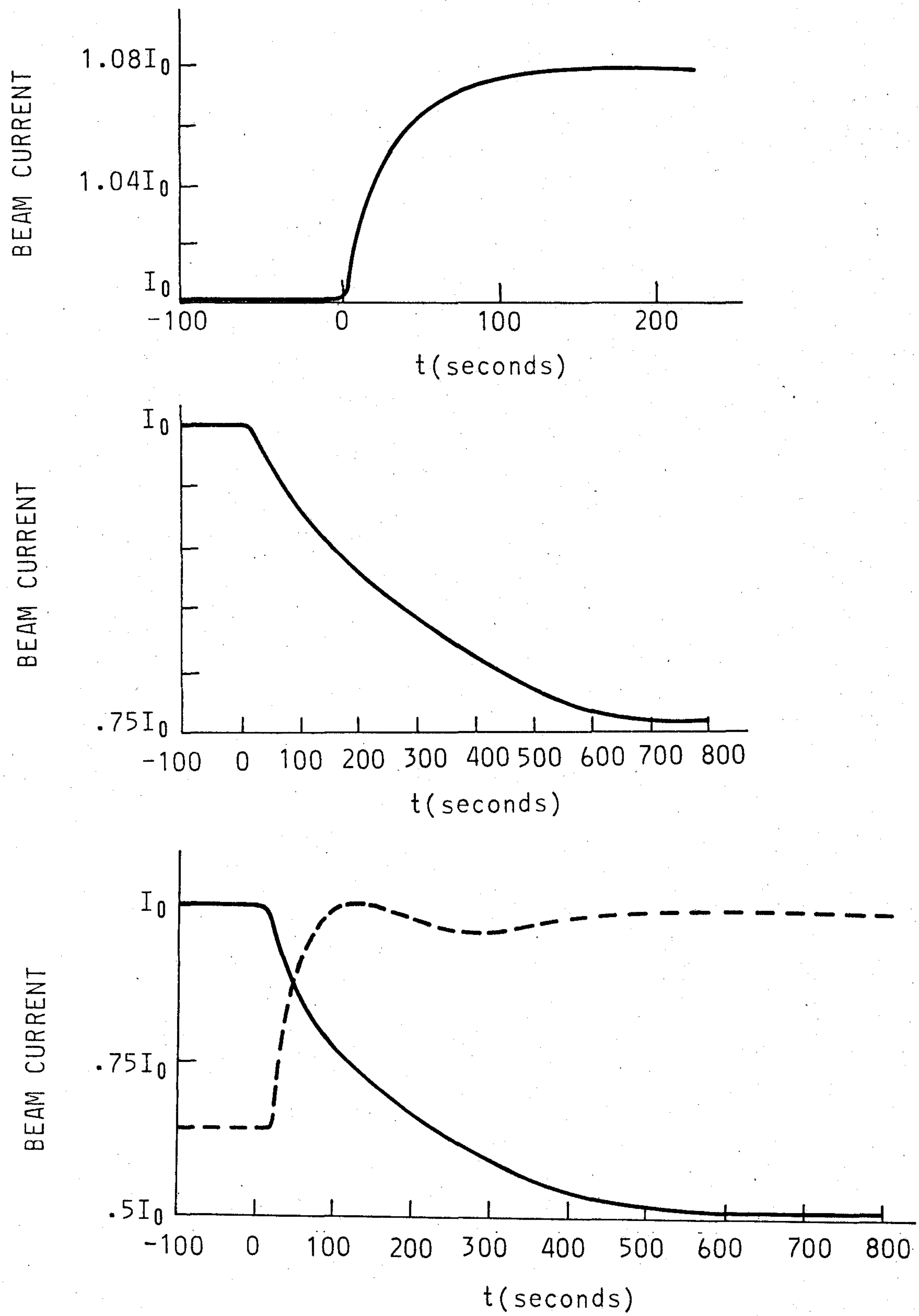

Fig. 24: Curves showing the response of the dispenser cathode emitted current to step function changes in heater current. Initial values of emitted current were greater than 100 mA.

appears that the dispenser cathode heater could be reduced in depth considerably without adverse effect on its operational or mechanical qualities.

In steady state operation the beam fluctuated $\pm 4\%$ over 10 minute intervals.

5.3 Foil Cathode

5.3.1 Preliminary Tests

An attempt was made to join a 0.127 mm thick tungsten foil to the molybdenum cathode by electron beam welding (Figure 8). In this process all of the material near the proposed weld is heated to a dark cherry glow. The beam current is then increased and the joint is heated to fusion temperature. The outer weld was not successful as differences in the thermal expansion of materials caused the foil to tear away from the cathode over half of the circumference. The inner weld also broke away in places but there was evidence that a bond could be made if the outer part of the foil was free to move radially. It is possible that the welding technique can be improved with practice and with proper materials selection. However, the high fusion temperature produces embrittlement of the tungsten foil, and any subsequent handling causes cracking.

To avoid the problems associated with welding, the foil was clampled to the cathode to permit testing of its mechanical properties and to find its temperature distribution. An annular molybdenum ring with a lip on it was press fit into the central hole sandwitching the foil underneath. The outer edge of the foil was held under a 0.5 mm thick molybdenum washer which was secured by three screws located as far as possible from the central hole.

In excess of 40 A was put through the tungsten foil while at a pressure of 10^{-2} P without significant heating. Since the resistivity of tantalum is three times that of tungsten (at $20^{\circ}C$) a 0.0046 mm thick tantalum foil

was clamped as before and tested. The tantalum, although thinner was much less brittle than the tungsten.
The optical pyrometer readings of foil temperature are tabulated below. It was impossible to attain the 2000°C required to get emission with the present power supply and feed through arrangement.

TABLE 4

OPTICAL PYROMETER READINGS

Radial Current (A)	Temperature ($^{\circ}$C)
25.0	835
30.0	900
40.0	975
43.5	1100

To heat the tantalum to 1100°C required current densities of 2.5×10^4 A/cm^2. This infers that a current density of approximately 7.5×10^4 A/cm^2 would be required in the tungsten foil to reach the same temperature. By comparison, measurements on a 0.025 cm diameter thoriated tungsten wire filament gave a temperature of 1100°C with 3.2×10^4 A/cm^2 and 1600°C with 6.4×10^4 A/cm^2. The current density in the tungsten foil was only 0.9×10^4 A/cm^2 which is a factor of eight below that required to reach 1100°C.

The time constant of the tantalum foil as measured by large temperature changes is less than half a second which is more satisfactory from a control point of view than the dispenser cathodes.

5.3.2 Discussion

The foil cathode arrangement discussed above has three fundamental problems. First, the large heat sink presented by the cathode body prevents the foil reaching operating temperature at reasonable currents. The second is the variation in radial current density causing non-uniform heating. For the very thin tantalum foil, heating was fairly uniform from the central nose which was thermally isolated, to the middle of the foil, but temperature dropped rapidly toward the outer edge. The third problem is the very thin foils required so that currents are not excessive. This is the most difficult problem to solve with the very simple arrangement in use here. Pulse transformers and electrical feedthroughs would require special design to handle the large currents required in the present design so alternate solutions must be found.

Since the mechanical properties of the tantalum foil cathode were good it would be possible to enlarge the outer radius of the foil considerably. This would increase the resistance of the foil and make the heat sink more remote from the emitting area. If small wedge shaped pieces were removed from the foil near the outer boundary, the current density could also be made more uniform.

A fine mesh could be used instead of the foil. This would certainly reduce the current requirement but it is not clear that the optics would necessarily be improved over the bifilar emitting filament presently in use.

An alternate solution would be to stretch the foil between two low mass concentric rings which would then be supported on small posts.

REFERENCES

1. J.R. Pierce, Journal of Applied Physics, 11, 548 (1940).
2. R. Helm, K. Spangenberg and L.M. Field, Electrical Communication 24, #1, 101 (1947).
3. J.R. Pierce, Theory and Design of Electron Beams, Van Nostrand, Priceton (1954).
4. R.A. Bonham and M. Fink, High Energy Electron Scattering, ACS Monograph, Toronto (1974).
5. R.O. Jenkins, Vacuum, 19, #8, 353 (1969).
6. H.J. Reich, McGraw-Hill Encyclopedia of Science and Tehcnology 14, 277 (1971).
7. R.B. Ayer, Proceedings I.R.E. 40, 591 (1952).
8. W. Kohl, Handbook of Materials and Techniques for Vacuum Devices, Reinhold, (1967).
9. R.O. Jenkins and W.G. Trodden, J. Electr. and Control 12, 1 (1962).
10. A.H. Beck, J. Electr. and Control 14, 623 (1963).
11. Semicon Associates Inc., Technical Bulletin, Lexington, Kentucky.
12. Philips Metalonics Technical Bulletin # B-51-27, Mount Vernon, N.Y.
13. J.B. Taylor and I. Langmuir, Phys. Rev. 44, 423 (1933).
14. J.H. deBoer, Electron Emission and Adsorption Phenomena, Cambridge (1935).

15. J.M. Lafferty, Journal of Applied Physics 22,#3, 299 (1951).

16. H.E. Gallagher, Journal of Applied Physics 40, # 1, 44 (1969).

17. H. Ahmed and A.N. Broers, Journal of Applied Physics 43, #5, 2185 (1972).

18. C. Sherman, Rev. Sci. Inst. 45, 1165 (1974).

19. H.P. Holloway and J.B. Hudson, Rev. Sci. Inst. 43, 828 (1972).

20. Private communication from Dr. E. Heighway.

21. W.B. Herrmansfeldt, Poisson Equation Solving Program, SLAC-51 CFSTI, National Bureau of Standards (1965).

22. A Guthrie, Vacuum Technology, John Wiley and Sons, New York (1965).

23. A.T. Nelms, National Bureau of Standards, Circular 577 (July 26, 1956).

24. T. Tabata, R. Ito and S. Okabe, Nuclear Inst. and Meth. 94, 509 (1971).

25. A Septier, Focusing of Charged Particles, Vol. 1, Academic Press, New York (1967).